1962

Angular Distribution of Satellite Scintillation

Joseph Kunkle Alexander
College of William & Mary - Arts & Sciences

ANGULAR DISTRIBUTION OF SATELLITE SCINTILLATION

A Thesis

Presented to

The Faculty of the Department of Physics

The College of William and Mary in Virginia

In Partial Fulfillment

Of the Requirements for the Degree of

Master of Arts

By

Joseph K. Alexander, Jr.

May 1962

APPROVAL SHEET

This thesis is submitted in partial fulfillment of

the requirements for the degree of

Master of Arts

L. K. Alexander Jr.
Author

Approved, May 1962:

James D. Lawrence, Jr., Ph.D.

John L. McKnight, Ph.D.

Robert L. Kernell, M.S.

F. R. Cromfield J/r

L E Smith

D E McLennan

Melvin A. Pittman

John W. Long

ACKNOWLEDGMENTS

The writer wishes to express his appreciation to Dr. J. D. Lawrence, under whose direction this investigation was performed, for his continued guidance and advice. The author is also indebted to Mr. J. D. Martin and Mr. William Hunt for their aid in acquiring and interpreting the data and to Miss Sharon Chapman and Miss Hope McDonnell for their assistance in reduction of the data. The writer also extends his special thanks to Miss Diana Titolo for her suggestions and help with the manuscript. This work was supported by the National Science Foundation under grant number NSF-G-16495.

TABLE OF CONTENTS

LIST OF FIGURES

ABSTRACT

Strip chart plots of signal strength versus time for the 54 mc/s transmissions of artificial earth satellite 1961 Omicron 1 are examined for transits over Williamsburg, Virginia, in the period October, 1961, to April, 1962. The random fluctuations in signal amplitude due to irregularities in ionospheric ionization density are interpreted with respect to satellite position. Amplitude scintillations show a marked dependence on elevation angle and appear to decrease to a minimum for elevations greater than 20°. The nature of scintillation at high angles of elevation (small zenith distance) is not clear. Occurrence of scintillation as a function of satellite azimuth shows clear north-south asymmetries with a maximum centered near magnetic north. The magnitude of scintillation increases sharply for latitudes above 40°N. These results indicate that the fluctuations observed depend upon the length of the ionospheric part of the propagation path and probably upon the angle between the direction of propagation and the earth's magnetic field.

ANGULAR DISTRIBUTION OF SATELLITE SCINTILLATION

INTRODUCTION

Historical Background

In 1946, Hey, Parsons, and Phillips[1] were studying cosmic electromagnetic noise radiation at 5 meters wave length when they observed short-period irregular fluctuations in the amplitude of noise power in the direction of Cygnus A. They concluded that these "scintillations" were due to variable emission of the cosmic radio source. In 1950, Smith[2] at Cambridge and Little and Lovell[3] at Jodrell Bank reported a series of observations of Cygnus and Cassiopeia at 3.7 and 6.7 meters. Observations of scintillation at the two stations separated by a distance of 210 km showed no correlation, whereas observations by receivers spaced within 4 km of each other showed good correlation. These results suggested that the fluctuations originated not in the source, but in the terrestial atmosphere and were most likely due to local changes in the refractive index of the ionosphere. Subsequent investigations of radio star scintillation were summarized by Booker[4] in 1958 with emphasis on the increase of scintillation with increasing zenith angle, the maximum occurrence of scintillation near midnight, and the correlation between amplitude scintillation and spread F reflections.

The development of artificial earth satellites made it possible to perform a more comprehensive study of the ionospheric irregularities responsible for scintillation phenomena. Slee[5], in 1958, reported observing fast, irregular fluctuations in the amplitude of the 108 Mc/sec signal from 1958 α (Explorer I). These scintillations occurred at a rate of about one cycle per second and appeared superimposed upon the regular

modulation caused by rotation of the plane of polarization at a linearly polarized receiving antenna. In 1959, Swenson and Yeh[6] concluded a 20 month study in which they recorded the 20 Mc/sec signals from 1957 α_2 (Sputnik I) and 1958 δ_2 (Sputnik III). They noted that night-time satellite scintillation appeared to originate at a height between 200 and 300 km and at latitudes north of 40° N. Daytime scintillation showed little geographical variation. They also suggested a correlation between the occurrence of satellite scintillation and spread F.

In the sections to follow some of the more important characteristics of that part of the terrestial atmosphere responsible for scintillations will be considered.

The Ionosphere

That portion of the upper atmosphere whose constituent gases are sufficiently ionized to affect the propagation of radio waves is designated the "ionosphere". Its lower limit is generally considered to be at an altitude of about 50 km, but its upper limit, although known to be above 500 km, is not well defined. Owing to the non-uniform density of ionization in the ionosphere, there exist stratified regions characterized by layers of relatively maximum ionization density. These regions are identified by the letters D, E, and F and differ in their origin and effect on radio waves. These regions and their ionization "peaks" are shown in Figure I which is a plot of average electron density versus height for a middle latitude, sunspot maximum, summer noon ionosphere.

One of the most widely used methods of studying ionospheric stratifications, particularly for the lower regions, is the sounding technique of reflecting pulsed radio signals from various heights. Short, radio frequency pulses which are variable over a wide frequency range are directed vertically or obliquely onto the ionosphere. From the time it takes for the pulse to be

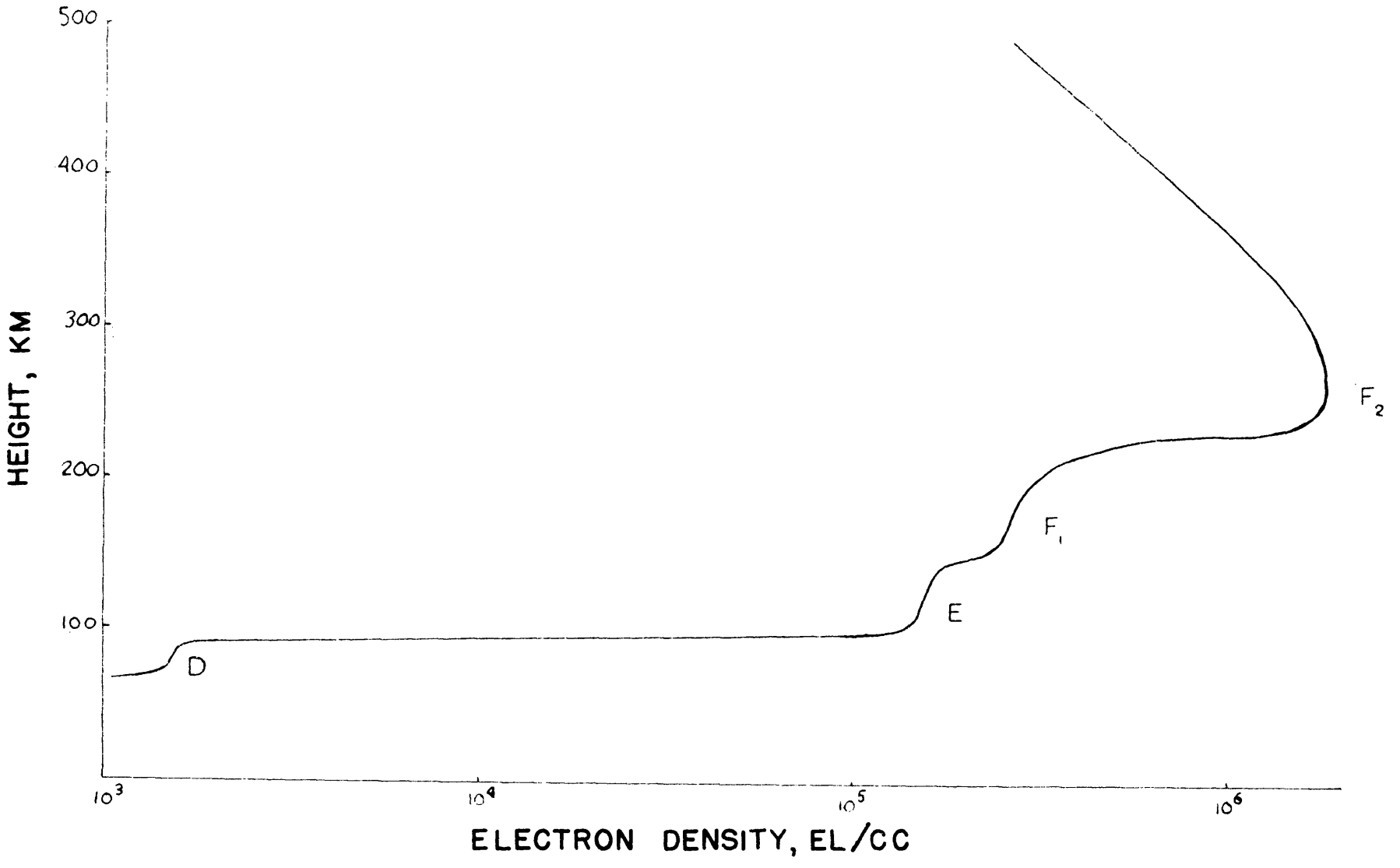

FIG. 1.- ELECTRON DISTRIBUTION IN THE IONOSPHERE

returned to a ground receiver, the height of the reflecting layer can be obtained. For vertical incidence, reflection will occur for all frequencies up to

$$\frac{4\pi N_e e^2}{m\omega^2} = 1.$$

For frequencies beyond this "critical frequency" $f_c = \omega_c/2$, transmission occurs. The maximum electron density for a particular layer may therefore be determined from

$$N_{max} = \pi m f_c^2/e^2.$$

These observations are usually presented in ionograms or ionosounds--plots of height on the vertical scale against frequency.

D Region

The lowest region, the D region, is generally considered to be that area between the altitudes of 60 and 90 km and is believed to have a daytime ionization maximum at about 80 km. The ionization layers of this region merge into the E layer at night but reform at sunrise over a period of little more than two hours. Aiken[7] has suggested that a major portion of the D-layer formation occurs during a 30-minute interval about sunrise, although radio investigations of the D-region diurnal changes do not all show such a marked effect.

Although the mechanisms involved in the formation of the D-region are not fully known, Nicolet[8] has suggested that the most important processes include ionization of O_2, Na, and NO. Aiken[7] has suggested a two-layer model of the D-region. In this theory, the upper layer, D_α, ranges between the heights of 80 and 100 km and is formed by Lyman-α ionization of NO by solar radiation. The lower D_β peak is situated at about 73 km and is formed by cosmic ray ionization.

Due to the strong influence of solar radiation in the formation of the

D layer, disturbances in this region generally accompany solar flares and related solar activity. Large scale fluctuations in the D region which occur during ionospheric storms are thought to cause "polar black-out" and sudden ionospheric disturbances (S.I.D.)[9]. The possibility that turbulence due to the formation of the D region near sunrise may create additional irregularities shall be examined later.

E Region

The next ionospheric level, the E region, is considered to lie in the altitude range from 90 to 140 km and possesses a midday ionization maximum of about 1.5×10^5 electrons per cm^3 at a height of about 110 km[10]. This layer is created primarily by ionization of molecular oxygen at the first and second levels[11]. It is important to note that at altitudes above 80 km photo-dissociation begins to break O_2 into atomic oxygen.

The E layer appears to experience strong solar influence - a characteristic that is effectively demonstrated by the diurnal variation if ionization density and correlation of the yearly variation of critical frequency with sunspot number[12]. The maximum electron density, N_mE, gradually begins to build up around sunrise from a night-time minimum until about an hour after noon and then decreases to the night-time level shortly after sunset. This cycle, however, is not as abrupt as that seem for the D layer. Information concerning the behavior of the normal E region at night is scarce and subject to question because of the occurrence of sporadic E. E region irregularities are also often observed in times of magnetic disturbances - particularly in the auroral zones.

Sporadic E

At times the region between 90 and 120 km exhibits random irregularities which are detected by abrupt increases in the critical penetration frequency. This phenomenom is called "sporadic E" or "Es" and is defined

by Smith[10] to be "comparatively strong and protracted transmission (several minutes to several hours) 'returned' from the E region of the ionosphere by some mechanism other than the normal reflection process from the daytime regular E layer." The structure of the Es layer is not clear; however, three models have been proposed to account for experimental observations - a thin horizontal layer situated within the regular E region, a steep gradient in the upper or lower part of the E region, and finally, scattering centers or blobs of ionization differing from the surrounding portions of the E region. Among the possible energy sources likely to cause sporadic E ionization are solar corpuscles (most probable in the auroral zones), meteors, thunderstorms, winds and turbulence, and ionospheric currents.

F Region

The F region is usually defined to be that part of the ionosphere above 150 km. During the day this region splits into two levels - the F_1 layer having a peak electron density at about 160 km and the F_2 layer with an ionization maximum around 250 km. At night, the F_1 layer appears to merge into the F_2 region, and the F_2 peak rises to an altitude around 350 km. Production of the F_1 and F_2 layers is most likely due to ionization of atomic oxygen although some ionization of N_2 may also be a contributing factor[11]. The greatest amount of ionospheric ionization occurs in the F region - the F_2 maximum electron density sometimes exceeding $1.8 \times 10^6/cm^3$.[13]

Disturbances in the F_2 region, usually in the form of a decrease in ioization density and an increase in layer altitude, are the primary causes of ionospheric storms. These irregularities, and most other F region fluctuations, appear to be closely associated with magnetic activity. Occasionally the echo reflected from the F region by sounding techniques shows a pulse of

a much longer duration that the incident pulse transmitted from the ground. This effect is called spread F and has shown considerable correlation with scintillation of the radiation from radio stars and artificial satellites[4,6].

Above the peak of the F_2 layer the electron density appears to fall off gradually although the ionization is thought to extend considerably beyond 500 km. This region cannot be reached by the usual sounding methods, and early studies had to depend on observation of "whistlers" and radiation from cosmic sources. Experiments utilizing artificial satellites are expected to contribute much new information concerning the behavior and composition of the upper ionosphere.

The Experiment

In these investigations, the radio signals of artificial satellite 1961 Omicron I (Transit IV-A) were examined for the presence of irregular fading of the received signal caused by a non-uniform electron distribution in the ionosphere. The 54 Mc/sec transmissions of Transit IV-A were recorded as plots of signal strength versus time at a station located near Williamsburg, Virginia (longitude 76°45' E, latitude 37°17' N), during the period from October, 1961, to April, 1962.

Before proceeding further, it is important that the meaning of scintillation as used in this paper, be clearly understood. When recorded, the undisturbed satellite signal appears as a sinusoidal trace having regularly occurring amplitude maxima and minima due to rotation of the plane of polarization of the radio wave. When a region of ionozation density irregularities exists between the satellite and an observer, irregular amplitude flunctuations will be noted due to variable refraction in the intermediate layers. By scintillation, therefore, we mean the random variations in signal amplitude caused by irregularities in the ionosphere.

The term "random" refers to both the rate and magnitude of the variations. By specifying that the fluctuations may be caused only by ionospheric irregularities, we mean to eliminate transmitted modulations, skip-distance focusing, and disturbances from thunderstorms, lightning, and ignition noise.

In this experiment the occurrence of scintillation was analyzed with respect to the parameters describing the position of the satellite relative to the observer - azimuth, elevation, and slant range. The variation of scintillation with latitude was also given special attention in order that a clearer picture of the "40° latitude cut-off" noted by other workers[6,14] might be established.

The elevation angle data is in substantial agreement with the similar investigation by Lawrence[14] and the results of star scintillation studies[4]. Scintillation activity increases for low angles of elevation, which seems to indicate that the ionospheric irregularities exist over a wide range of altitudes. The data for high elevation angles is not clearly understood.

A maximum amount of scintillation appears near the azimuth of magnetic north, and scintillation is more predominant west of the observer than east of the observer. These properties strongly suggest a relation between the earth's magnetic field and the irregularities responsible for scintillation. Latitude studies agree with earlier observations and affirm the relation between scintillation and the magnetic field. Scintillation increases considerably for latitudes north of the observing station, but occurs only weakly at latitudes south of the observer. Further studies of the variation of scintillation with azimuth and latitude should offer much information concerning the magnetic properties of the ionospheric irregularities.

EQUIPMENT

1961 Omicron I - Transit IV-A[15,16]

The launching of the 1961 Omicron payload with a Thor-Able Star rocket in late June, 1961, was of special significance since it represented the first successful orbital injection of three satellites at the same time and the first launching of a device carrying a nuclear auxiliary power unit. Mounted on top of Transit IV-A in "piggyback" fashion were 40-pound Injun and 55-pounds Greb III. The two smaller satellites, instrumented to gather data on solar radiation, auroral zones and related phenomena, were separated from the parent device by explosive bolts and springs but failed to separate from each other.

The 175-pound Transit is equipped with a thermoelectric generator measuring five inches in diameter and 5.5 inches in length. The heat generated by the spontaneous decay of a small amount of Plutonium 238 is converted into electrical energy by thermocouples. In this manner, the low voltage, high current device supplies the satellite instruments with 2.5 watts of power.

Transit is a polygon of 16 sides - 43 inches in diameter and 31 inches high - with a flat top and bottom. It is equipped with radio transmitters at 54 Mc/sec and 320 Mc/sec, two of which are nuclear powered, and two of which are powered by solar cells located on the surface of the satellite. The 54 Mc/sec Doppler signal is phase modulated by approximately 35° with a ring type modulator. The antenna configuration may be seen in Figure 2 which shows the 1961 Omicron payload assembled for launch. Transit IV-A has a nodal period of 103.8 minutes, an inclination of 66.8°, an apogee altitude of 997 km and a perigee altitude of 880 km.

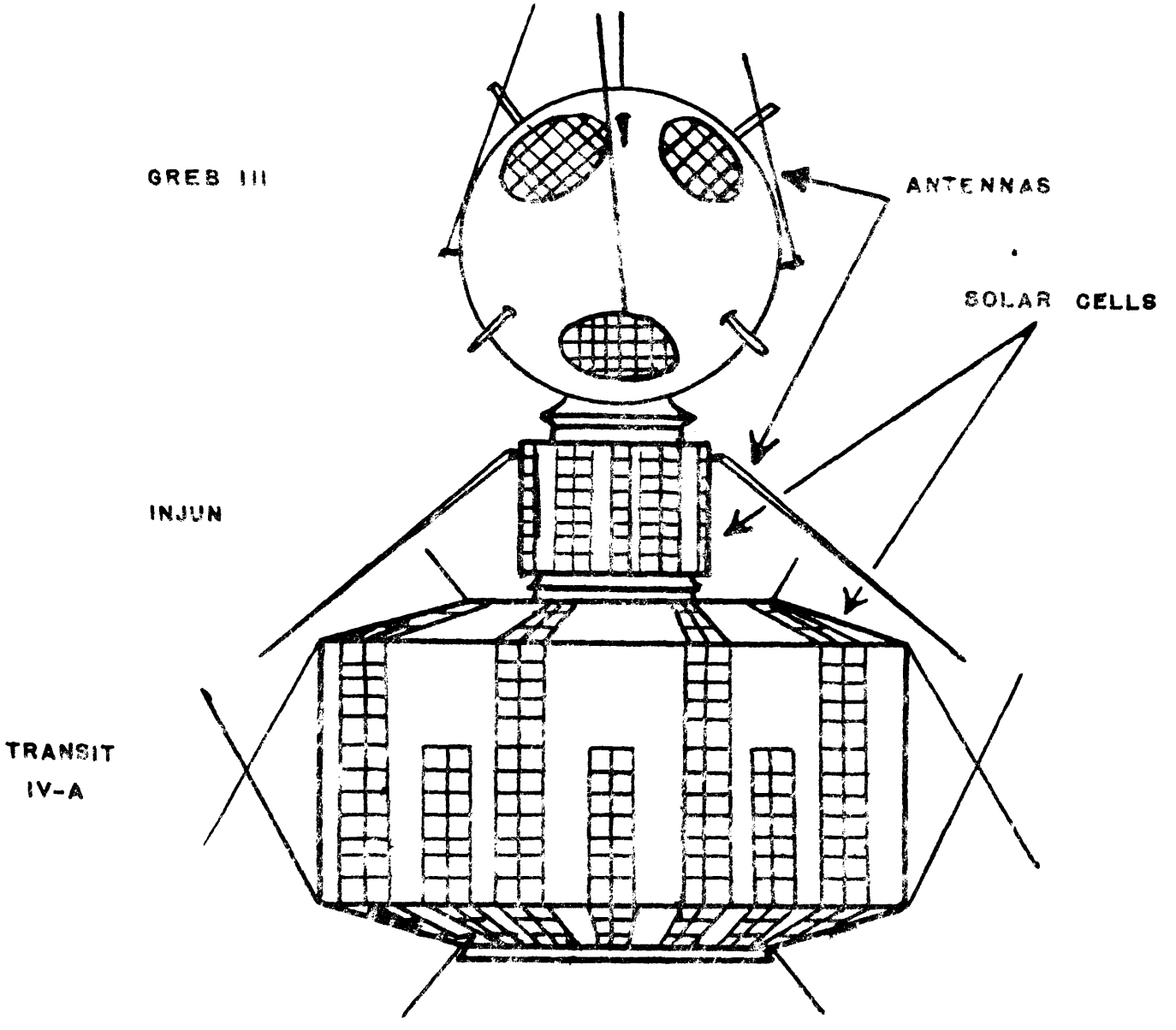

1961 OMICRON ASSEMBLED FOR LAUNCH

FIGURE 2.

The satellite is designed to provide a new and accurate time standard more dependable than WWV whose signal is subject to variable ionospheric refraction. Orbital information will be fed from ground stations to the satellite magnetic memory system every 12 hours; the transmitter will then broadcast its precise position over the earth 11.18 seconds. Broadcasts will be triggered by a frequency divider composed of 25 transistorized circuits controlled by a highly stable 3,000 kc/sec crystal oscillator.

Receiving and Recording Equipment

The satellite signal was taken from a half-wave folded dipole antenna to a Tapetone pre-amplifier-convertor to produce an intermediate frequency of 14.4 Mc/sec which was fed to a Collins 51J-4 receiver. The signal at the receiver detector was sent to a cathode-follower, integrated, and then fed to the amplifier of a Brush strip-chart pen recorder. A block diagram of the satellite receiving equipment is shown in Figure 3, and the individual components of the system will be discussed in the sections to follow.

Antennae

The receiving antennae used for satellite observations were half-wave folded dipoles made of 300 ohm, heavy duty twin lead (Amphenol 214-185). The overall length of the half-wave sections is given by

$$L_o = EC/2f ,$$

where C = velocity in free space, E = end correction factor[17] = 0.95, and f = frequency. The length of the folded section is given by

$$L_1 = VEc/2f ,$$

where V(=0.84) is the velocity factor for 300 ohm twin lead. The difference between the total antenna length and the length of the folded section was corrected by adding a short piece of heavy copper wire to each end of

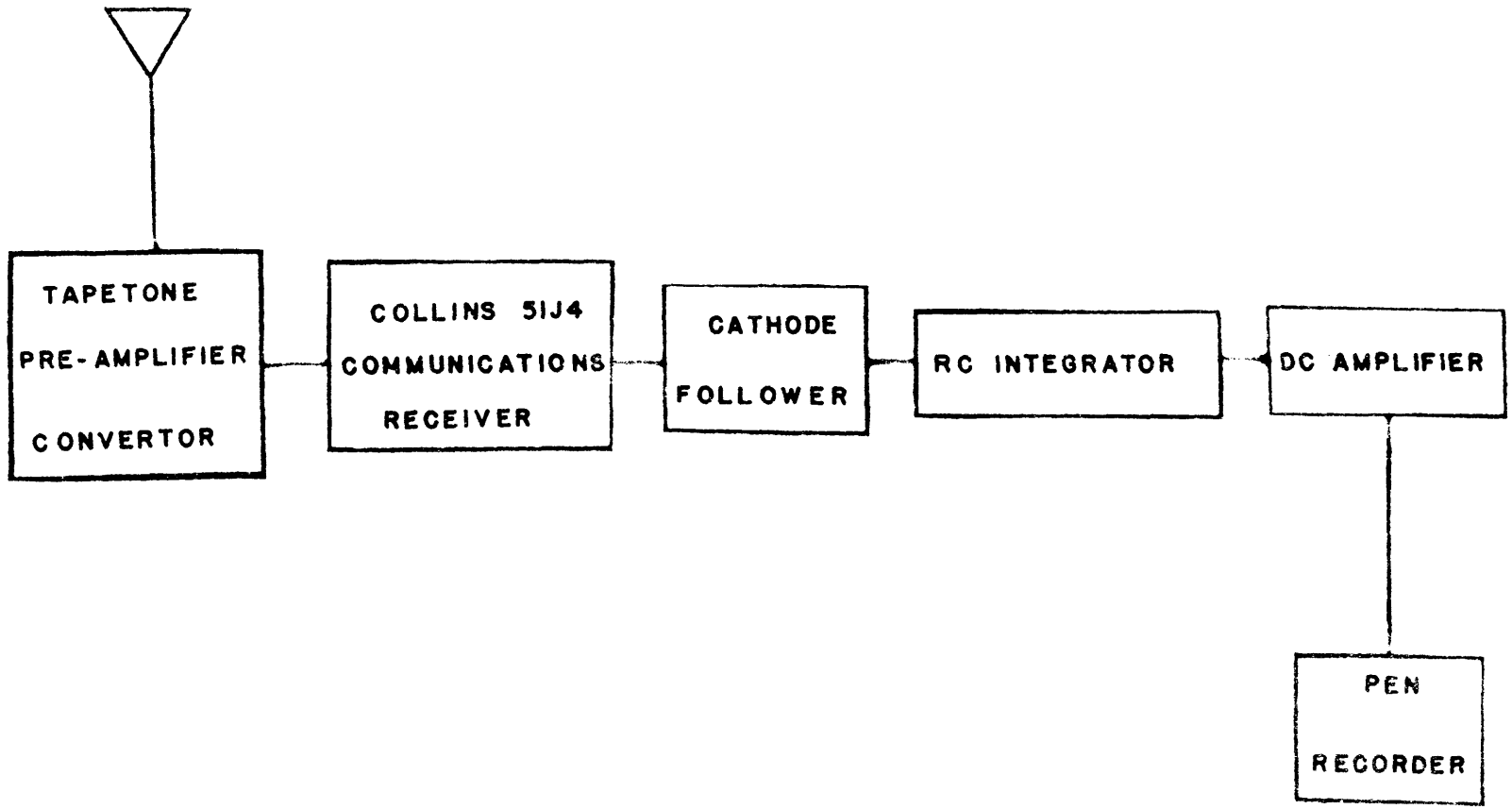

BLOCK DIAGRAM OF RECEIVING EQUIPMENT

FIGURE 3.

the folded section. To provide a proper impedance match to the 73 ohm coaxial lead-in (RG-59/U), a half-wave balun of RG-59/U coaxial cable was used as shown in Figure 4. The velocity factor for RG-59/U was taken to be 0.66.

The antennae were suspended approximately 27 feet above ground between aluminum masts. Glass insulators on the ends of the dipoles were connected to $\frac{1}{4}$ inch diameter nylon cord which was fed through pulleys atop the masts to the ground. This system facilitated changing antennae. Four sets of masts were situated in such a manner that two pairs of perpendicular antennae could be used at one time. Each pair of crossed dipoles was oriented so that one was aligned in a north-south direction and the other in an east-west direction with their midpoints coincident. By using dipoles at right angles to one another, one could observe the rotation of the plane of polarization of the satellite signal.

The folded half-wave horizontal dipole, having a linear polarization, has the advantage of minimizing the interference from terrestrial radiation near the horizon and is simpler to construct than more expensive and complex high gain antennae. Placing the antennae at a considerable height above the ground reduces the effect of obstructions on the ground. This advantage outweighs concern over the minor distortions in an ideal ground plane introduced by guy wires and masts needed to support the antennae at this height.

Converter

A Tapetone TC-54 crystal-controlled frequency converter was used to convert an input frequency of 54 Mc/sec from the antenna to an intermediate frequency of 14.4 Mc/sec. This convertor employs a pair of 6BQ7A tubes as a cascode RF amplifier, a 6CB6 mixer stage, and a 12AT7 tube in the crystal-controlled local oscillator. The TC-54 has a noise figure of

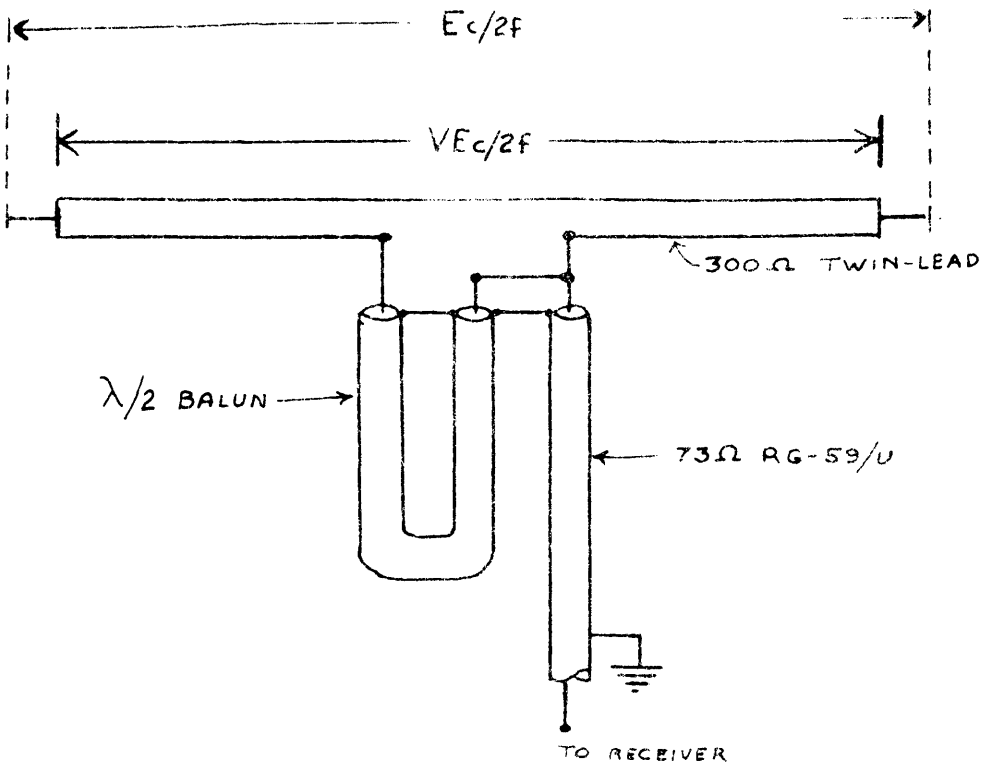

FIG. 4.-RECEIVING ANTENNA

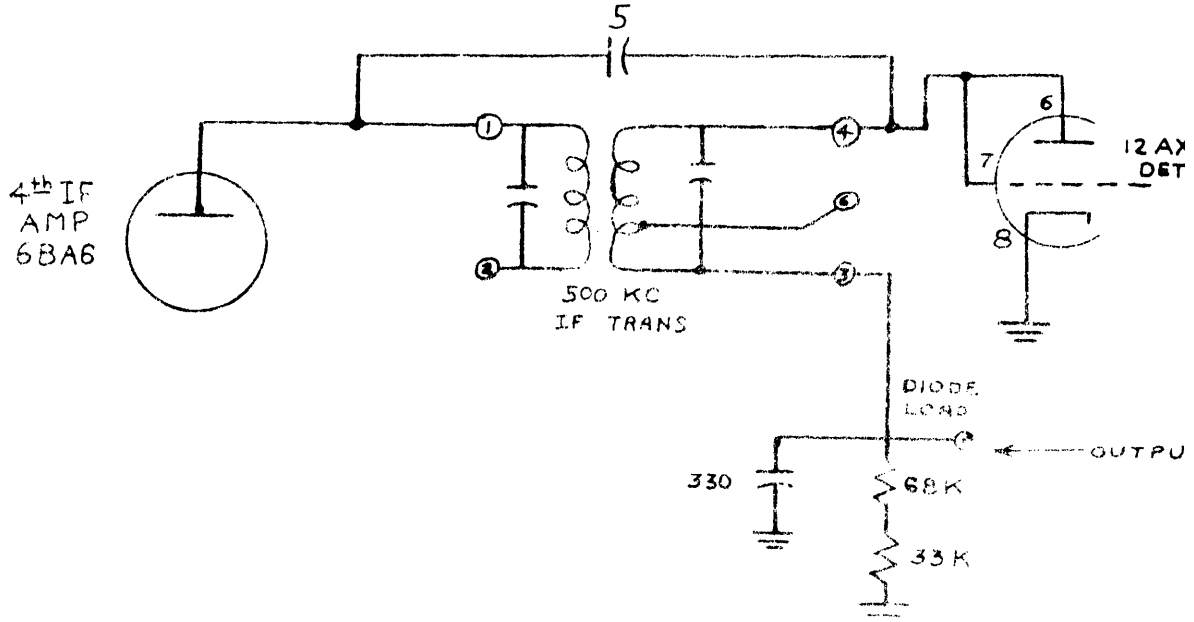

FIG. 5.-5IJ-4 OUTPUT LOCATION

3.2 db, a power gain of 44db, and an overall band-width of 1.0 Mc/sec. Its performance when used with a 51J-4 receiver is shown in Figure 6. A circuit diagram is given in Appendix I.

Receiver

Two Collins 51J-4 Communications Receivers were used to detect and record the satellite transmissions. The Collins 51J-4 Receiver is a highly stable and accurate superheterodyne receiver which employs single, double, and triple conversion to tune the frequency range of 540 kc/sec to 30.5 Mc/sec in 30 one-megacycle bands for AM or CW reception. Each band is covered in ten turns of the tuning dial which is calibrated at 100 kc/sec intervals. A total setting error and drift of less than 1 kc/sec is possible and calibration at room temperature will assume frequency stability within 300 cps. The sensitivity is such that less than 5μv gives a signal-to-noise ratio of 10 db.

In the frequency range of interest, 13.5 to 14.5 Mc/sec, the signal receives one stage of r-f amplification and is then applied to the grid of the first mixer to produce a variable i-f frequency of 2:5 to 1.5 Mc/sec when beat against the high frequency oscillator controlled by the second harmonic of a 8 Mc/sec crystal. The 2.5 to 1.5 Mc/sec variable i-f signal is then combined at the grid of the second mixer with the output of the highly stable 3 to 2 Mc/sec permeability turned variable frequency oscillator to produce a fixed 500 kc/sec i-f. Three stages of i-f amplification follow. Additional features of the 51J-4 receiver include a crystal filter for improved selectivity, a low impedance AVC, two stages of audio amplification, and a 100 kc/sec frequency spotter and/or calibrator.

Mechanical i-f filters are used to provide band-width steps of

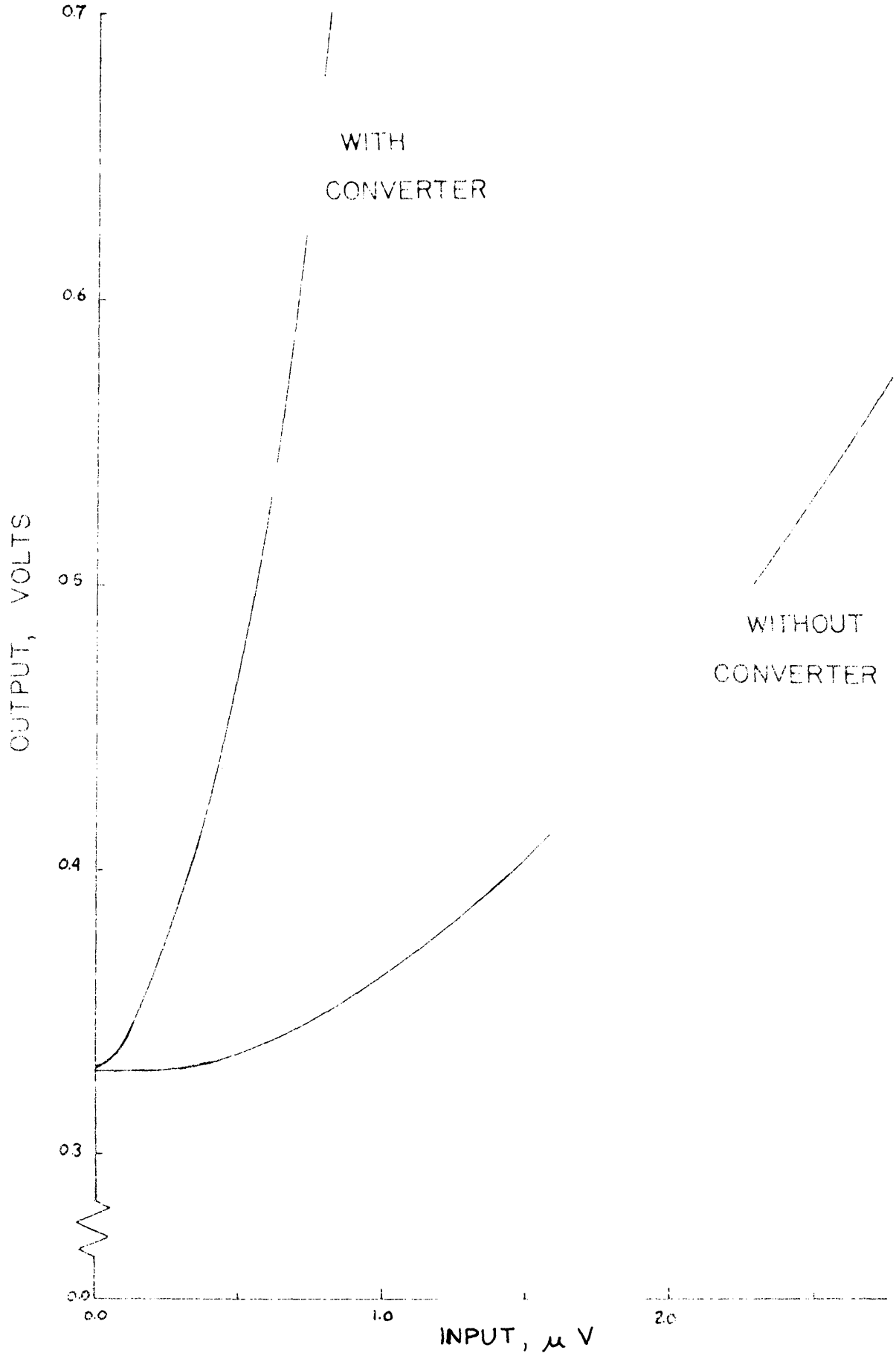

FIG. 6.- INPUT VERSUS RECEIVER OUTPUT

1 kc/sec, 3 kc/sec, or 6 kc/sec. For the 54 Mc/sec transmissions of Transit IV-A, a 3.1 kc/sec mechanical filter is used. This filter passes a band of frequencies approximately 3 kc/sec wide and is centered on 500 kc/sec.

The detector of the 51J-4 receiver consists of one half of a 12AX7 dual triode tube. The grid is connected to the plate so that the tube may be used as a diode with rectification taking place between the plate and the cathode. The signal voltage to be recorded after integration is taken from the Diode Load test point above a 100k load resistance in parallel with 330$\mu\mu$f for r-f filtering. This test point is located in Figure 5.

Input versus receiver output data in the operating range for satellite observations are shown in Figure 6. The lower curve gives the performance of the receiver alone at 14.4 Mc/sec with a 3 kc/sec band-width and an r-f gain setting of 8. With maximum r-f gain, the receiver noise figure measured with a hot diode noise source and a 50 ohm load resistor is 15. The upper curve shows the combined performance of the 54 Mc/sec converter and the receiver with a 3 kc/sec band-width. In the range of interest, the combination has a total r-f gain of about five million and a noise figure of about 2.5.

Integrator

In order to prevent amplification of frequencies higher than the linear response of the recording system, the signal from the receiver is integrated. The signal from the detector is first fed to a cathode follower which is used to present a constant impedence to the detector output. From the cathode follower, the signal goes to a simple RC integrator and then to the Brush DC amplifier as shown in Figure 7. The cathode follower has a voltage gain of nearly one and a maximum output

FIGURE 7. - CATHODE FOLLOWER AND INTEGRATOR

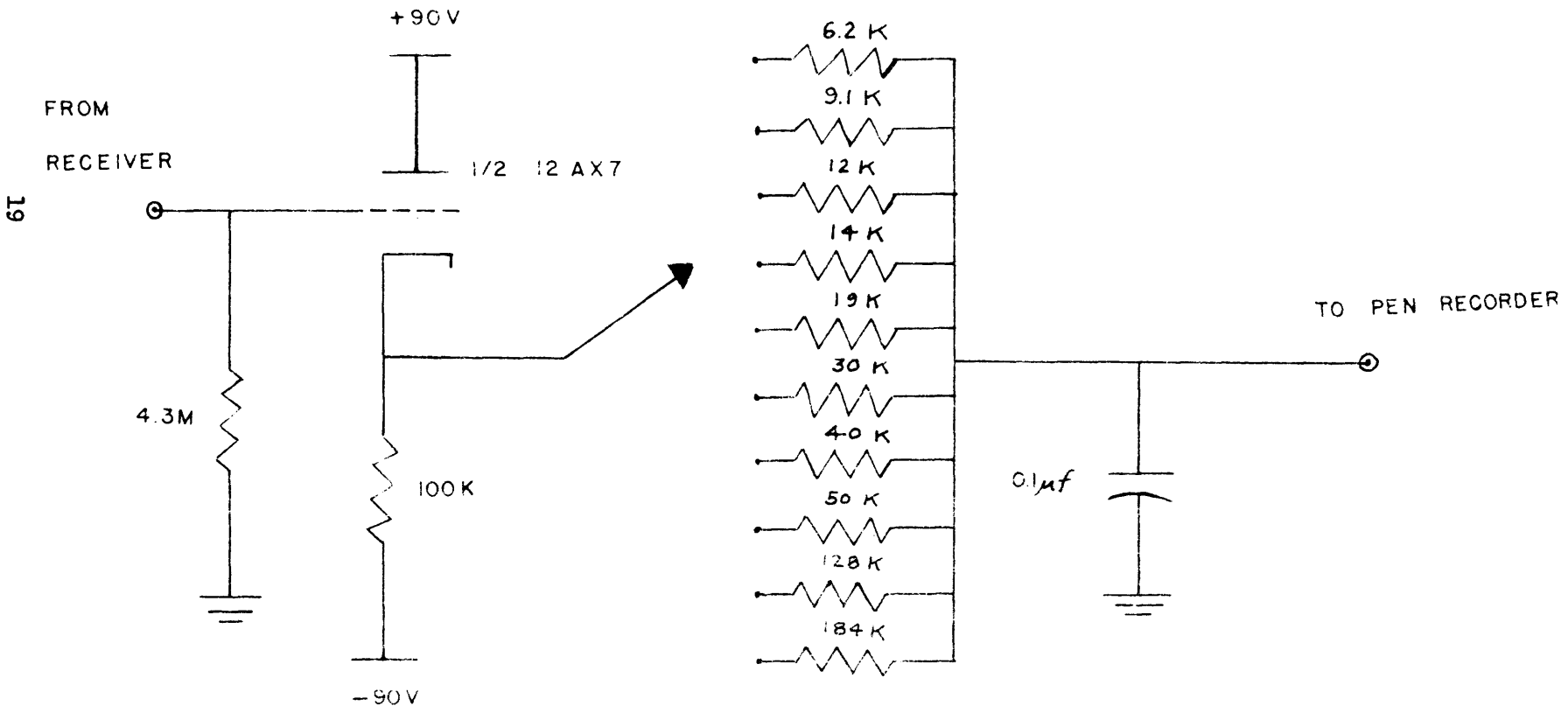

of about 2.0 volts[14].

Recording Equipment

The integrated signal is fed to a four-channel Brush Pen Recording System, Model RD-2641-00. This recording system includes DC amplifiers (Model RD-5211-03) which provide sensitivity steps of 0.01, 0.02, 0.05, 0.1, 0.2, 0.5, 1, 2, 5, and 10 volts per chart line (mm). This range of DC amplification permits full-scale measurements from 0.40 volts to 400 volts. The oscillograph pen motor has a DC sensitivity of 1.5 volts per chart line (mm) or 30 volts full scale from center. The frequency response is such that the peak to peak amplitude of a constant voltage sine wave can be recorded within $\pm\frac{1}{2}$ chart line of a nominal 40 lines from DC to 10 cps or within ± 1 line of a nominal 10 lines from DC to 100 cps. The maximum amplitude is 40 lines to 40 cps and 10 lines to 100 cps. Chart speeds are regulated by a direct-drive synchronous motor, and speeds of 1, 2, 5, 10, 25, 50, 125 and 250 mm/sec are available.

Auxiliary Equipment

In addition to the two Collins 51J-4 receivers used for reception of the satellite signals, a Hallicrafters SX-42 receiver and a Hallicrafters SX-62A receiver were used for monitoring other frequencies and for WWV reception. For most records, the SX-62A was used with only a single-wire antenna to record the WWV time signal at 2.5 Mc/sec or 5.0 Mc/sec. Although severe fading of WWV or highly disturbed propagation conditions sometimes made it impossible to record the WWV code, the operator could place an accurate timing mark on the chart by noting the audio signal.

Data Acquisition

The technique of obtaining satellite records was quite straightforward and simple. From the information on the NASA orbit prediction bulletins the time at which a satellite could be expected to rise above the observer's

horizon was estimated within ±30 seconds. After the recorder amplifiers and the receivers were given sufficient warm-up time and were calibrated, the operator located the satellite signal by tuning with the receiver BFO on or by watching the recorder trace while searching at the satellite frequency. Due to the sharp selectivity of the 51J-4, occasional retuning was necessary during a pass to follow the Doppler frequency shift. This amounted to about one kilocycle for each 20 Mc/sec of transmitted signal. Since the satellite could not be tracked with a fixed dipole antenna, the gain of the system was not constant. In order to record as much of the pass as possible from horizon to horizon, the recorder gain was changed when necessary to keep a clear record on the chart. Every effort was made to hold these changes to a minimum.

PROCEDURE

Satellite Records

Satellite transits were recorded on strip charts in the form of plots of signal strength versus time. Chart paper was usually fed at a rate of 10 mm/sec for Transit IV-A passes which had an average duration of 15 minutes.

The signal strength traces varied in a quasi-sinusoidal manner due to the rotation of the plane of polarization of the radio wave as observed with a linearly polarized antenna. This rotation was due to bodily rotation of the satellite, which meant a rotation of the transmitting antenna, and due to the ionospheric Faraday effect, which will be discussed in the section to follow. Rotation of the satellite would appear to occur at a constant rate throughout a transit whereas the rate of Faraday rotation varied with the position of the satellite.

Scintillation appeared in the form of random amplitude fluctuations which, in extreme cases, varied as much as 100% from the undisturbed signal level. The rate of scintillation varied from 0.2 cps to as much as 5 cps. For most observations, signal strength recordings from two perpendicular antennae were placed on adjacent channels. Amplitude variations due to rotation of the plane of polarization would then be detected by the phase difference between the two channels during most of the record. Scintillations, however, would appear simultaneously on both traces. The National Bureau of Standards timing signal from station WWV was recorded on a third channel.

Faraday Rotation

The two components of a linearly polarized radio wave, in the general

case, travel with different velocities and are elliptically polarized with opposite senses. When the direction of propagation is parallel to the earth's magnetic field and the wave frequency is much greater than the gyromagnetic frequency and plasma frequency of the ionosphere, the ordinary and extraordinary waves become circularly polarized. The resultant is a linearly polarized wave whose plane of polarization is gradually rotated due to the differing phase velocities of the two components. When the direction of propagation is perpendicular to the earth's field both elliptically polarized components become linearly polarized. The resultant gradually changes from linear polarization to circular and back to linear polarization again due to the different velocities of the two components. The plane of polarization of the resultant undergoes a rotation by $\pi/2$ during each cycle. This rotation of the plane of polarization of a radio wave as it travels through the ionosphere is known as the ionospheric Faraday effect.

It can be shown (Appendix II) that if one assumes a direction of propagation at small angles from the earth's magnetic field and a frequency sufficiently larger than the plasma and gyromagnetic frequencies, the rotation of the plane of polarization may be given by

$$\phi = \frac{K}{f^2}\int NB \cos\Theta \, dl ,$$

where K = a constant

f = transmitted frequency

N = electron density

B = earth's magnetic field strength

Θ = angle between magnetic field and propagation path

dl = element of path length along line of sight l.

For small zenith angles δ, this may be written

$$\phi = \frac{K}{f^2} \langle B\cos\theta \sec\delta \rangle_{av} \int_0^h N dz ,$$

where B, $\cos\theta$, and $\sec\delta$ are averaged over the ionospheric part of the path. Differentiation with respect to time gives the rate of rotation of the plane of polarization. Bowhill[18] has shown that with certain assumptions (see Appendix II) this becomes

$$\frac{d\phi}{dt} = \frac{K N_T B_x V}{f^2 h} ,$$

where N_T = the integrated electron density

B_x = component of magnetic field parallel to satellite motion

V = velocity of satellite

h = satellite height.

Scintillation Indices

In order to describe the magnitude or severity of the amplitude fluctuations in the satellite signal due to ionospheric irregularities, a set of "scintillation indices" has been developed. The indices occur in half-integral steps from 0.0 to 2.0 to conform with those suggested by Swenson and Yeh[6]. A particular record is divided into ten-second intervals, and each interval is assigned an index by inspection. The intermediate indices developed by Lawrence[14] have been incorporated to provide a closer description of the degree of scintillation, but since the Lawrence indices have been subjected to some modification they will be described in detail. Examples of the scintillation indices for the 54 Mc/sec signal of Transit IV-A are shown in Figure 8.

Index 0.0

When scintillation is absent the records only show the regular fading which is characteristic of an undistrubed ionosphere. This condition is associated with the index 0.0. The first two examples in

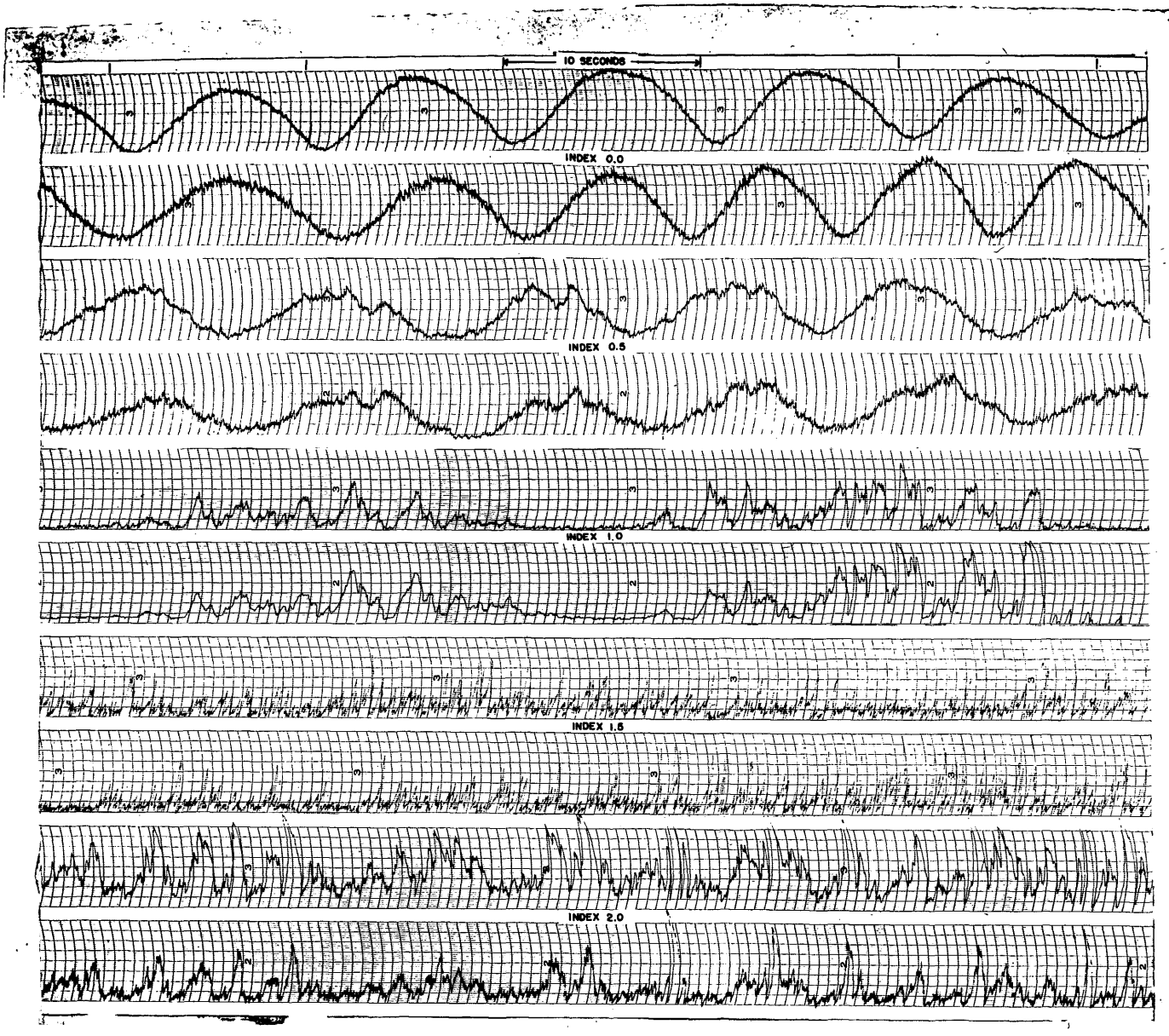

SCINTILLATION INDICES – TRANSIT IV-A

FIG. 8.

Figure 8 show typical portions of a Transit IV-A daytime record having index 0.0.

Index 0.5

The index 0.5 is meant to be roughly equivalent to the index 0.33 suggested by Lawrence. In this case the Faraday rotation is still clear; however, small amplitude fluctuations may be seen superimposed upon the regular envelope. The second pair of records in Figure 8 illustrate this index. In the two examples recorded simultaneously by crossed antennae, it should be noted that the scintillations occur at the same time in each record although the Faraday periods are slightly out of phase.

Index 1.0

In many cases, the satellite signal suffered sharp, random amplitude variations as shown in the third pair of records in Figure 8. This condition is assigned an index of 1.0 and is considered to be indicative of significant irregularities in the ionosphere. Although the Faraday fading can still be distinguished, the irregularities are much deeper than in the case for index 0.5. As before, the example shows that the scintillations were coincident for both receivers.

Index 1.5

The index 1.5 is meant to replace the index 1.33 described by Lawrence and is often characteristic of the signal for large zenith angles, i.e., when the satellite is farthest from the receiver. In this case, the signal is considerably weakened although occasional strong "bursts" are noted. Faraday rotation is no longer evident. The fourth pair of samples in Figure 8 show the presence of 1.5-type scintillation at two different times.

Index 2.0

Records showing the most severe type of scintillation are assigned

the index 2.0 and are thought to represent a highly disturbed ionosphere. This is noted by the presence of violent variations in the signal which often completely obscure the Faraday rotation. The scintillations are of large amplitude and usually occur at a rapid rate. Index 2.0 is illustrated in the last pair of records in Figure 8. Again the correlation of scintillations between two antennae at right angles is very clear.

Although this system of indices is not foolproof, it is thought to give a fairly good picture of how the ionosphere affects the radio signal. Since the indices are assigned by inspection, some variation in analysis is possible due to the individual interpretation of a particular experimenter. Some discrepancy is also possible for different amounts of signal amplification and recorder sensitivity. A constant gain system is, therefore, highly desirable. With proper care, however, these minor disadvantages are not serious, and any radio signal may be examined with this technique provided it is free from complicated modulations.

Satellite Orbits

Since, to a first approximation, the gravitational field of the earth may be considered to vary radially as the inverse square of the distance from the center of the field, the orbit of a satellite may be described by the Keplerian form of an ellipse having one focus at the center of the earth. Due to the earth's equatorial bulge, regions of variable crust thickness and gravitational anomalies, the satellite orbit varies slightly from an ellipse having a fixed plane and major axis predicted by the central field approximation. Higher order spherical harmonics in the gravitational potential function give rise to a precession of the orbit plane about the polar axis of the order of 3-4 degrees per day in a sense opposite to that of the orbital motion[19].

The essential orbit geometry is shown in Figure 9. OP is the polar axis and OQ is the orbit axis. The orbit inclination, i, is the space angle between the orbit plane and the earth's equatorial plane. Due to the earth's west to east rotation about the polar axis, an observer at latitude L will pass through the orbit plane twice each sidereal day provided $L<i$. The solar times at which the satellite may be observed will move backwards about 4 minutes per day due to the motion of the earth about the sun. Adding to this the daily time difference due to precession of the orbit causes the orbit plane to cross the observer about 12-15 minutes earlier each day.

In describing the motion of a satellite about the earth it is often useful to consider the sub-satellite locus - the intersection of the orbit plane with the surface of the earth. The points at which the sub-satellite curve cuts the equator are called nodes - the ascending node being the point directly below the satellite as it crosses the equator going from south to north. The nodal period of a satellite, therefore, is the time between two successive crossings of the equator and is on the order of 100 minutes for a typical satellite. Periods of less than 90 minutes are impractical since they require that the satellite move at such a low altitude that drag forces would prevent the existence of a stable orbit.

In view of the above considerations, a satellite may be expected to make a close pass by an observer (within 1000 miles) about 3-6 times in a 24 hour period. For observers for which $L>i$, this number will be less, of course. Corresponding nodes of consecutive orbits will move westward 20-30 degrees each revolution.

Map Overlay Method

Determinations of pass times and satellite azimuth, elevation, and

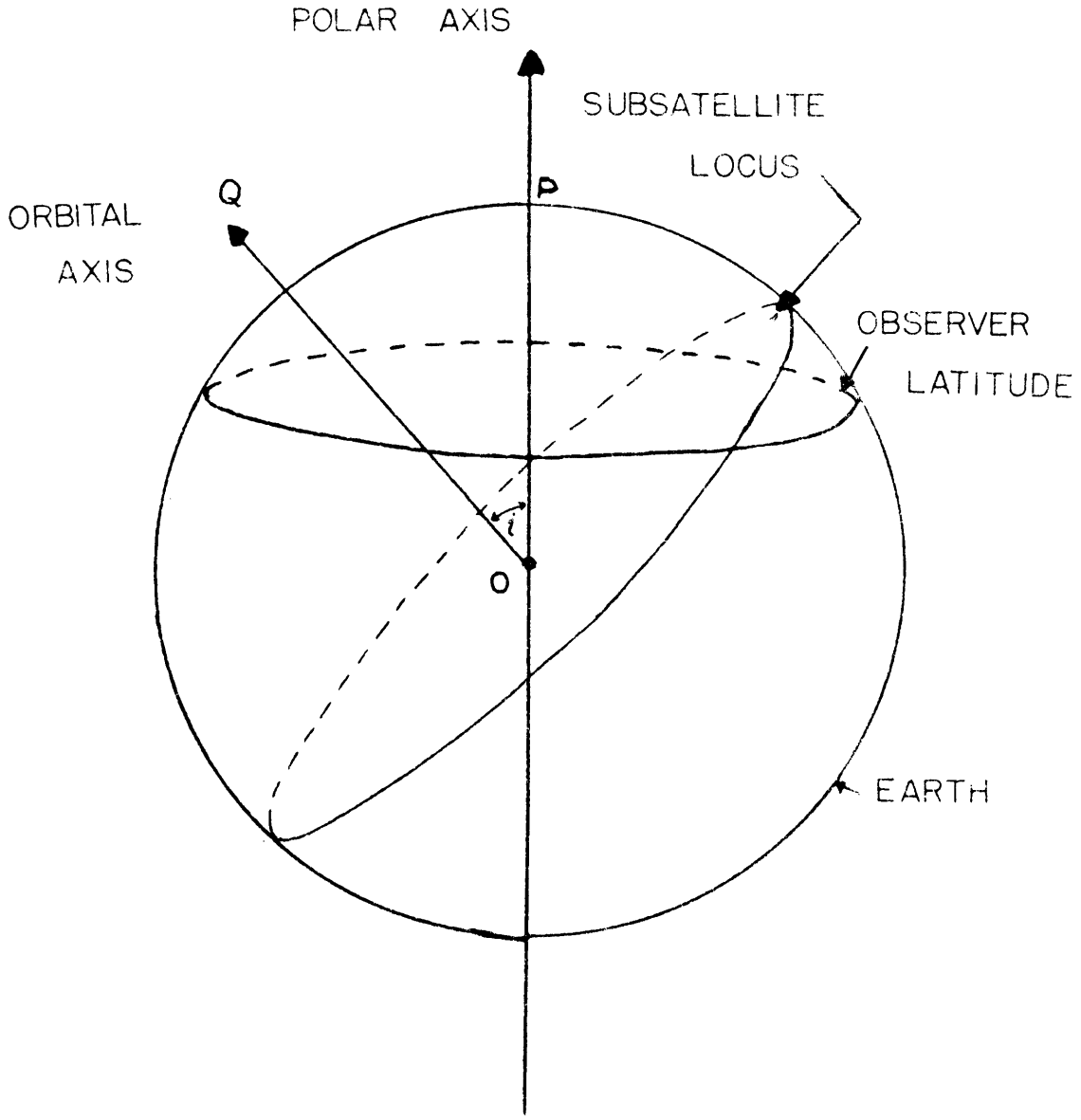

SATELLITE - OBSERVER RELATIONSHIP

FIGURE 9.

slant range for intervals during a particular transit were made by employing a two-dimensional projection of the world and the satellite prediction bulletins issued by Goddard Space Flight Center of NASA. This simple technique is known as the "map overlay method". A set of concentric circles 150 miles apart was drawn around the observer's position on a large Miller cylandrical projection of the world out to a distance of 2100 miles. These curves, termed "acquisition circles", determine the distance from the observer to a particular sub-satellite point.

A transparent acetate sheet the same size as the world map was used to construct the sub-satellite plot. (In practice, only that part of the sub-satellite plot in the northern hemisphere was constructed). After an equatorial line was traced on the sheet the sub-satellite plot could be drawn readily from the latitude-longitude information in the prediction bulletin. A third section of the bulletin enabled an observer to obtain the time after equator-crossing and height of the satellite for points along the plot. By placing the origin of the sub-satellite plot over the longitude of the ascending node for a given pass as predicted in the NASA bulletin, an observer could establish the satellite position for any time during the transit. The satellite azimuth could be obtained by inspection and the elevation and slant range could be determined by referring to a chart which reduces the necessary computations to graphical form. For a satellite such as Transit IV-A having a relatively stable orbit, a single acetate overlay could be used for over a month before the trajectory changed sufficiently to change the sub-satellite plot.

EXPERIMENTAL RESULTS

A total of seventy-nine records of artificial earth satellite 1961 Omicron 1 were examined and analyzed for the presence of scintillation. A list of the passes used and pertinent data concerning the trajectories is given in Table 1. Scintillation indices were assigned to the records in ten-second intervals and the satellite height, slant range, latitude, azimuth, and elevation were determined for each minute during a pass. Position information for shorter time intervals could then be obtained by interpolation. In the sections to follow, the occurrence of scintillation is studied with respect to elevation, azimuth, and latitude.

Elevation

As one might expect, scintillation activity shows a rather marked dependence upon elevation angle - especially when the satellite is near the horizon. A histogram of scintillation index averaged over five degree elevation intervals for all passes and all azimuth angles is shown in Figure 10. Maximum scintillation occurs near the horizon and decreases steadily as the elevation increases to about 20°. The fluctuations observed during this portion of a pass were usually of the type having an index 1.5. For elevations above 20° the scintillation activity appears to "level out" at a steady minimum. The sharp increase in average index for elevations above 65° which appears in Figure 10 is not entirely understood but may be attributed to several causes. First, the number of observations available for study varies inversely with elevation angle since only the very close transits afford data near the zenith. In view of this, the data for high elevations may not represent a

TABLE 1

SUMMARY OF DATA

Date	Time of Pass (GMT)	Revolution No.	Long. of Asc Node
10-5-61	0222	1358	182.83
10-5-61	0408	1359	250.90
10-7-61	0256	1386	196.58
10-8-61	2003	1410	105.50
10-11-61	2045	1452	126.12
10-13-61	0418	1470	237.81
10-23-61	2350	1620	208.59
10-26-61	2254	1661	203.00
11-20-61	1625	2004	191.38
11-20-61	1805	2005	217.59
11-20-61	1956	2006	243.79
11-21-61	1638	2018	198.25
12-4-61	1610	2198	234.82
12-15-61	1329	2349	231.78
1-22-62	1958	2880	106.66
1-25-62	1855	2921	101.07
1-26-62	1728	2934	81.73
1-31-62	1649	3003	89.88
2-1-62	1702	3017	96.75
2-2-62	0209	3022	227.77
2-6-62	1442	3085	78.69
2-6-62	1628	3086	104.89

TABLE 1 (Continued)

Date	Time of Pass (GMT)	Revolution No.	Long. of Asc Node
2-7-62	0136	3091	235.92
2-9-62	0018	3118	223.45
2-9-62	1525	3127	99.30
2-10-62	1540	3141	106.17
2-11-62	2314	3159	217.86
2-12-62	1421	3168	93.71
2-14-62	1451	3196	107.33
2-15-62	1318	3209	87.99
2-16-62	1333	3223	94.86
2-18-62	1402	3251	108.60
2-20-62	1243	3278	96.14
2-21-62	2205	3297	234.04
2-22-62	1125	3305	883.68
2-22-62	1508	3307	136.09
2-23-62	2047	3324	221.57
2-27-62	1058	3374	91.82
2-28-62	1106	3388	98.69
3-1-62	1842	3406	210.38
3-2-62	2042	3421	243.46
3-3-62	1002	3429	93.10
3-6-62	1807	3475	218.52
3-7-62	1821	3489	225.39
3-9-62	0944	3512	108.10
3-15-62	1643	3599	227.93
3-16-62	0606	3607	77.57
3-19-62	1555	3654	229.12

TABLE 1 (Continued)

Date	Time of Pass (GMT)	Revolution No.	Long. of Asc Node
3-20-62	0516	3662	78.76
3-20-62	1422	3667	209.78
3-20-62	1607	3668	235.99
3-22-62	0545	3690	92.49
3-23-62	0558	3704	99.36
3-25-62	0442	3731	86.89
3-26-62	0457	3745	93.75
3-27-62	0510	3759	100.61
3-28-62	0337	3772	81.27
3-28-62	0524	3773	107.48
3-29-62	1301	3791	219.17
3-29-62	1445	3792	245.37
3-30-62	1313	3805	226.03
3-31-62	0421	3814	101.88
4-3-62	0317	3855	96.27
4-4-62	0146	3868	76.93
4-4-62	0332	3869	103.14
4-5-62	1109	3887	214.82
4-5-62	1249	3888	241.03
4-10-62	0125	3951	91.92
4-10-62	1032	3956	222.95
4-10-62	2355	3964	72.59
4-11-62	0140	3965	98.79
4-12-62	0007	3978	79.46
4-12-62	0154	3979	105.66
4-12-62	1102	3984	236.69

TABLE 1 (Continued)

Date	Time of Pass (GMT)	Revolution No.	Long. of Asc Node
4-13-62	0930	3997	217.35
4-17-62	0120	4048	113.80
4-17-62	0839	4052	218.62
4-19-62	0001	4075	101.40
4-20-62	0736	4093	213.09
4-21-62	0030	4103	115.15

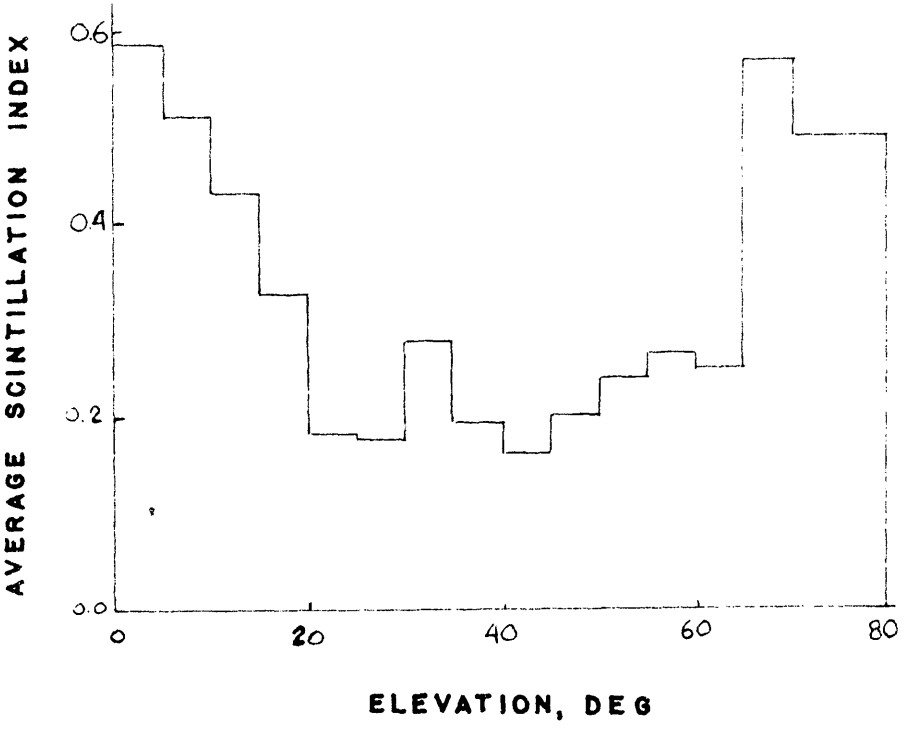

FIGURE 10.— AVERAGE SCINTILLATION INDEX VERSUS ELEVATION

legitimate statistical sample, and this fact could produce an unreasonable average index. A second explanation may exist in the fact that the apparent velocity of the satellite when nearly overhead is greater than when near the horizon. Consequently, as the source passes more rapidly over the ionospheric irregularities the fading rate comes more rapid. In a number of cases, the fading rate is so high (6 cps) that regular Faraday fading is indistinguishable. This could lead an observer to assign an index to that portion of a record which would be larger than justified by the real level of the scintillation.

The plots shown in Figure 11 show the variation of the scintillation index with elevation angle for 20-degree azimuth intervals. The dotted sections of the plots indicate intervals of inadequate data. Most plots clearly show the elevation effect. The azimuth interval 181° - 200° is a notable exception, however, and may be explained by the fact that little scintillation is seen at any elevation. This decrease in scintillation activity south of the observer shall be considered later. The apparent increase in scintillation index with high elevation angles for the azimuth intervals 181° - 340° may be due, in part, to poor statistics as has already been mentioned.

Azimuth

The variation of scintillation with satellite azimuth angle is shown in Figure 12 which gives the scintillation index for ten-degree azimuth intervals averaged over all elevations. The most striking feature of this plot is the distinct scintillation maximum centered just to the west of true north. This maximum is more nearly coincident with magnetic north which is also displaced a few degrees west of true north. A minimum amount of scintillation appears to occur around 130° east. A relative east-west asymmetry can also be seen with a higher average

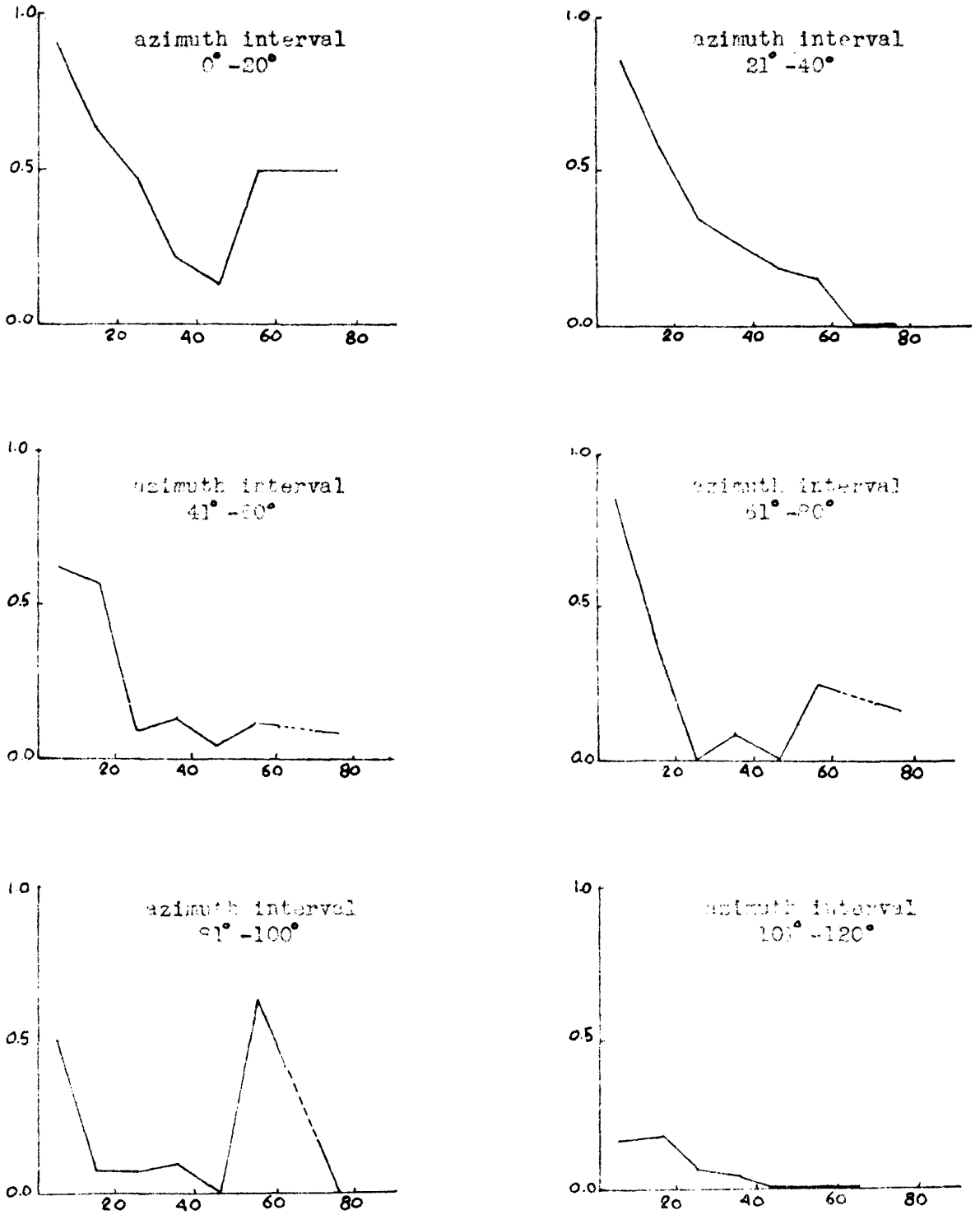

AVERAGE SCINTILLATION INDEX VERSUS ELEVATION

FIGURE IIA.

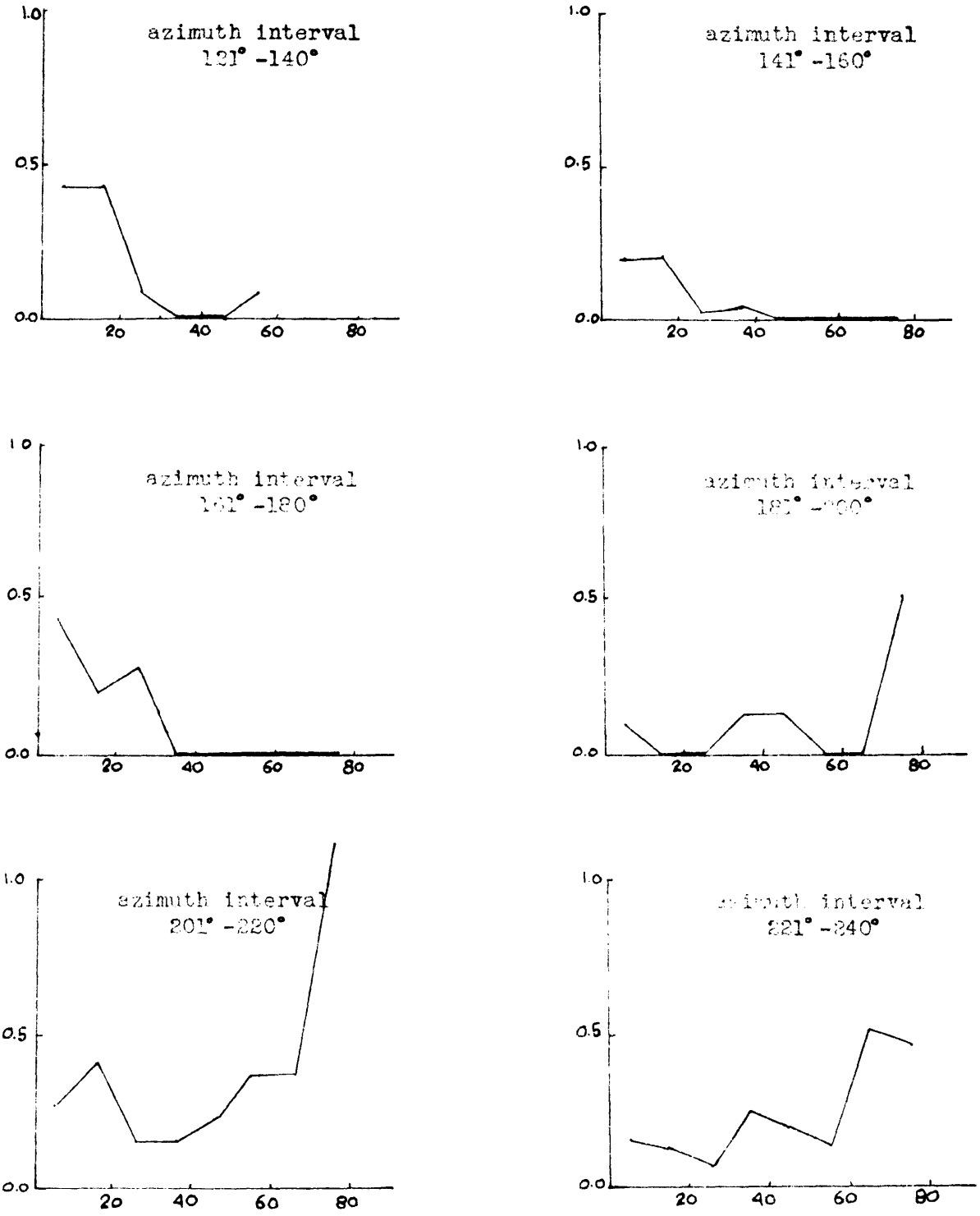

AVERAGE SCINTILLATION INDEX VERSUS ELEVATION

FIGURE 11B.

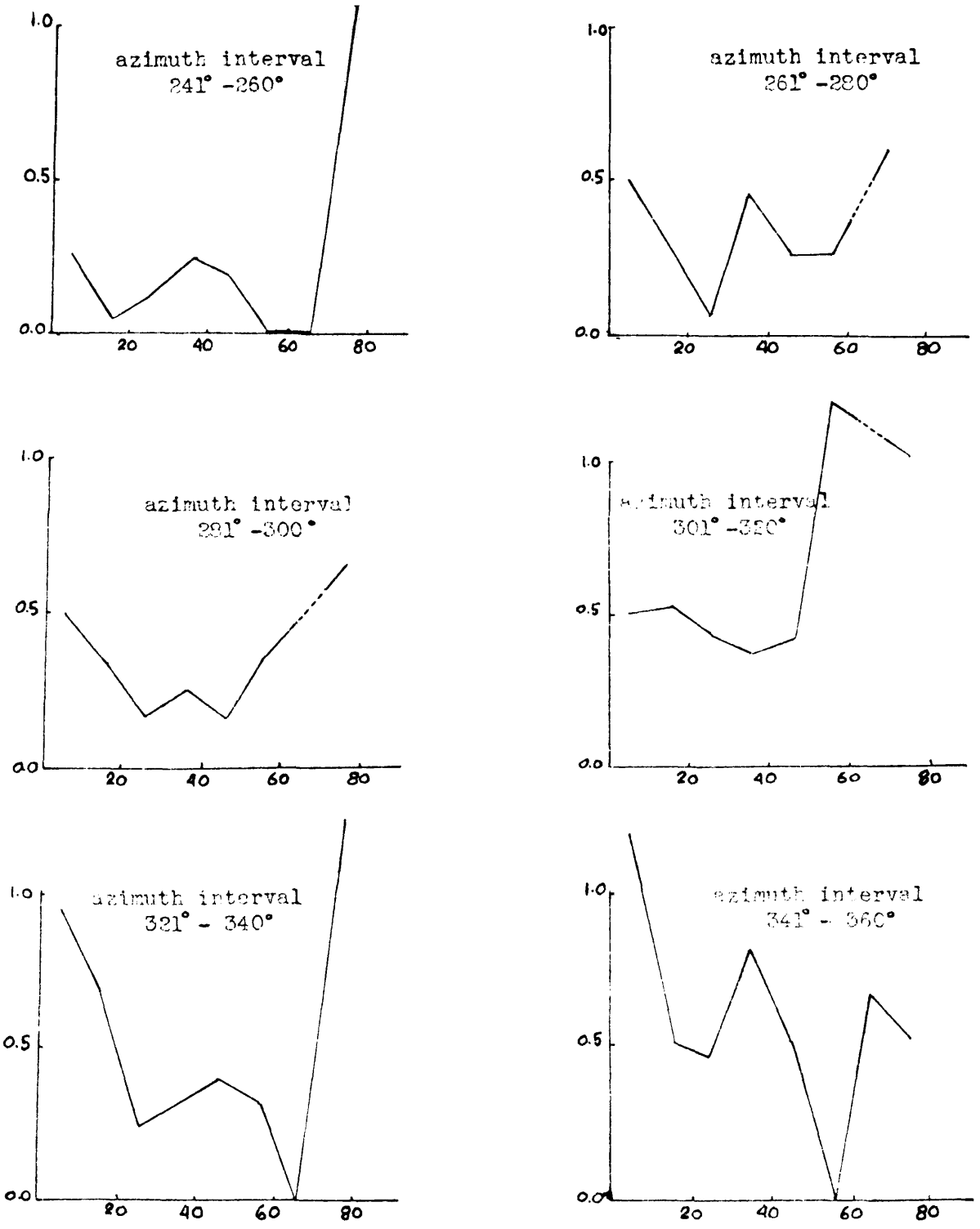

AVERAGE SCINTILLATION INDEX VERSUS ELEVATION

FIGURE IIC.

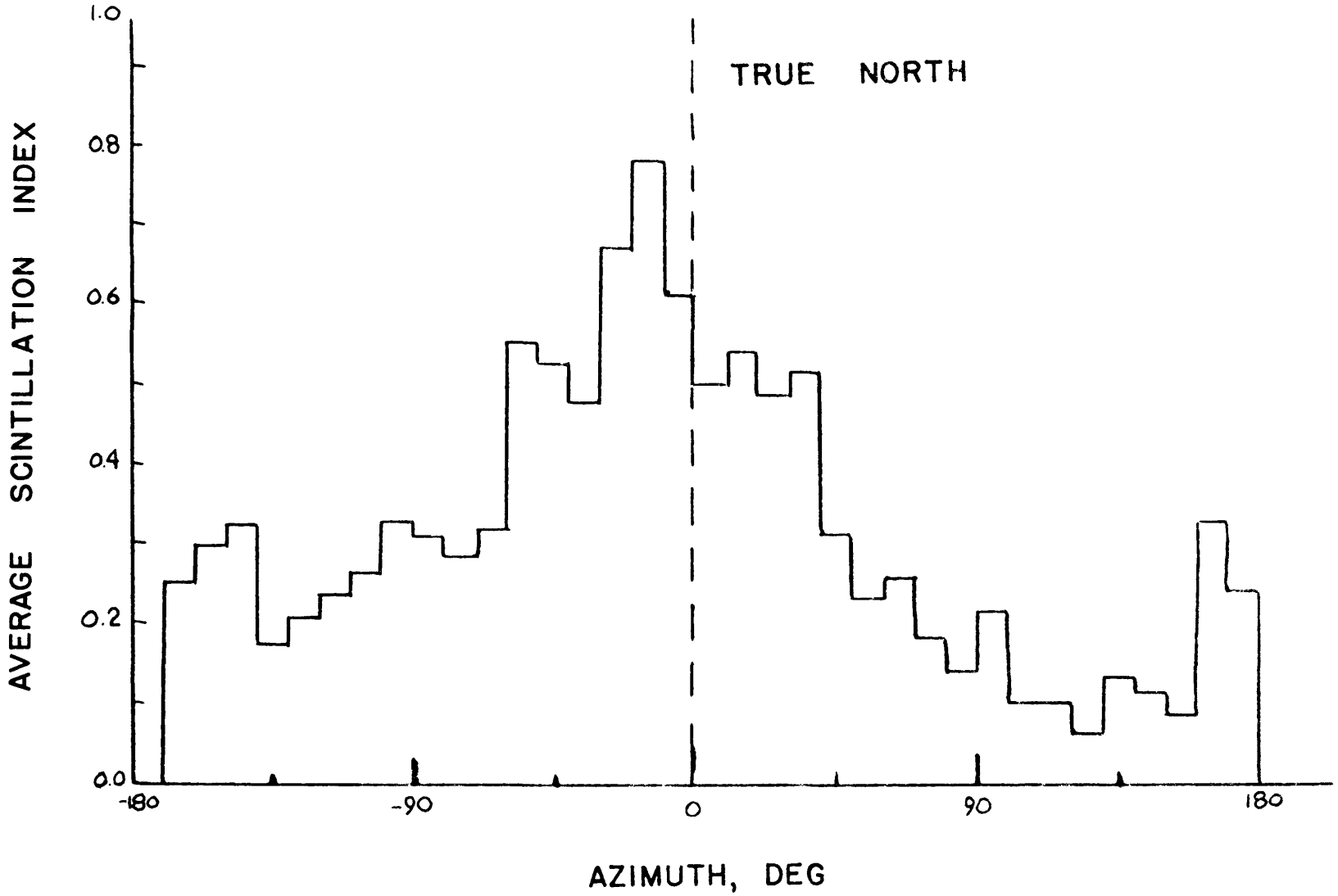

FIGURE 12.- AVERAGE SCINTILLATION INDEX VERSUS AZIMUTH

scintillation index at -90° than at +90°. This is in close agreement with the results obtained by Lawrence[14]. In both experiments the average index at -90° is about 50% higher than at +90°.

Plots of average scintillation index versus azimuth angle for ten-degree elevation intervals are given in Figure 13. The relative maximum near magnetic north may be seen in each of the plots up to an elevation of about 50°. The last three plots show little regularity in the occurrence of scintillation as a function of azimuth. This again may be due to the inadequacy of the data for high elevation angles.

Latitude

Special attention has been given to the variation of scintillation with the latitude of the satellite, and these results are given in Figure 14. The secondary peak of the average scintillation index in the region between 13°N and 21°N is probably not indicative of a latitude effect but is primarily an elevation effect. When the satellite is this far south, it is near the horizon, and therefore, more scintillation is observed. From 25° to about 34°N the average scintillation index has a nearly constant minimum value. The average index begins to increase gradually just south of the observer's latitude and shows a steady increase from about 42°N up to a maximum at the most northerly latitude at which the satellite may be observed. Although much of the scintillation for latitudes above 55° may be due to the elevation effect, a definite north latitude effect appears to exist. This may be related to the azimuthal variations of scintillation and their association with the earth's magnetic field.

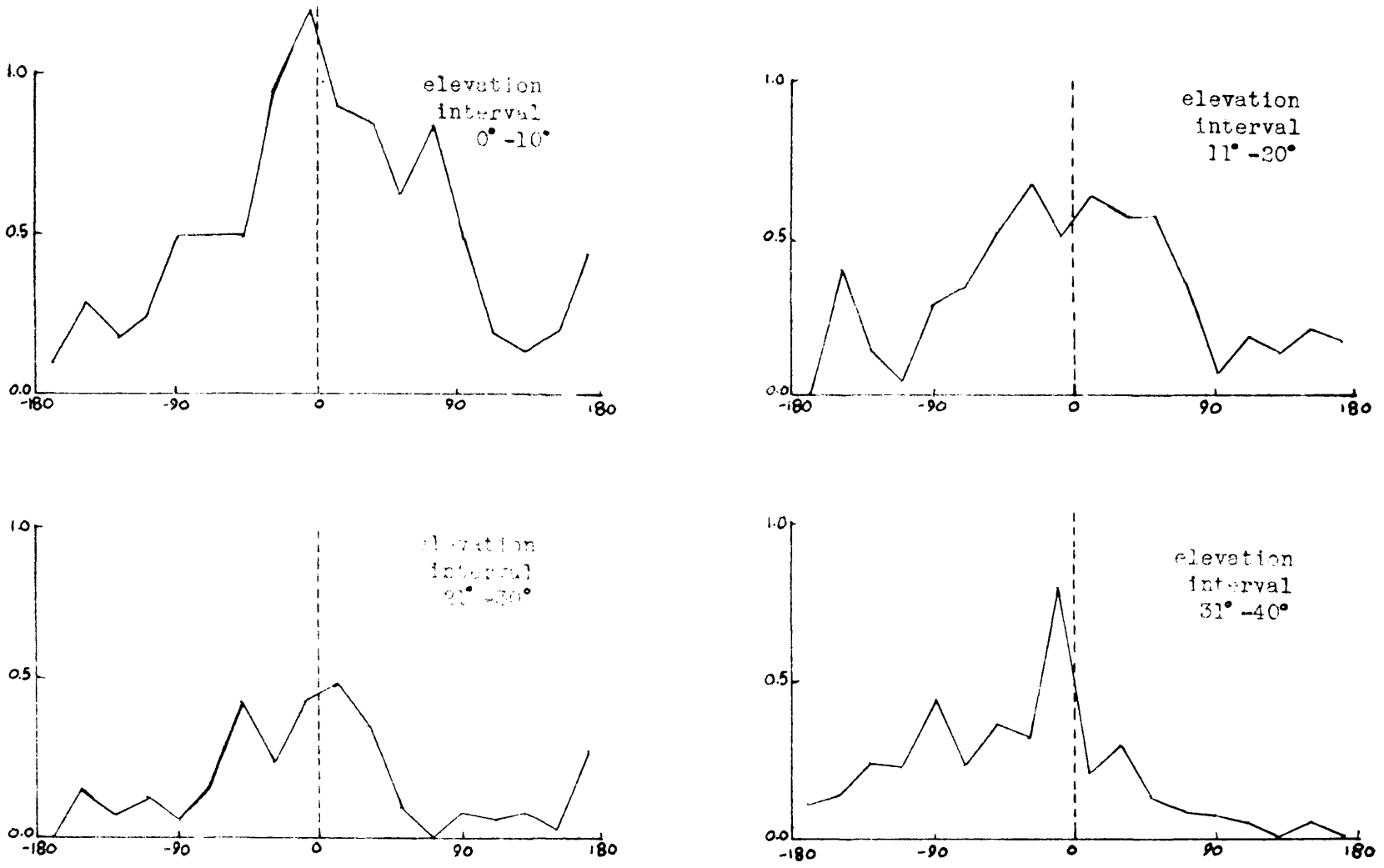

FIGURE 13A.- AVERAGE SCINTILLATION INDEX VERSUS AZIMUTH

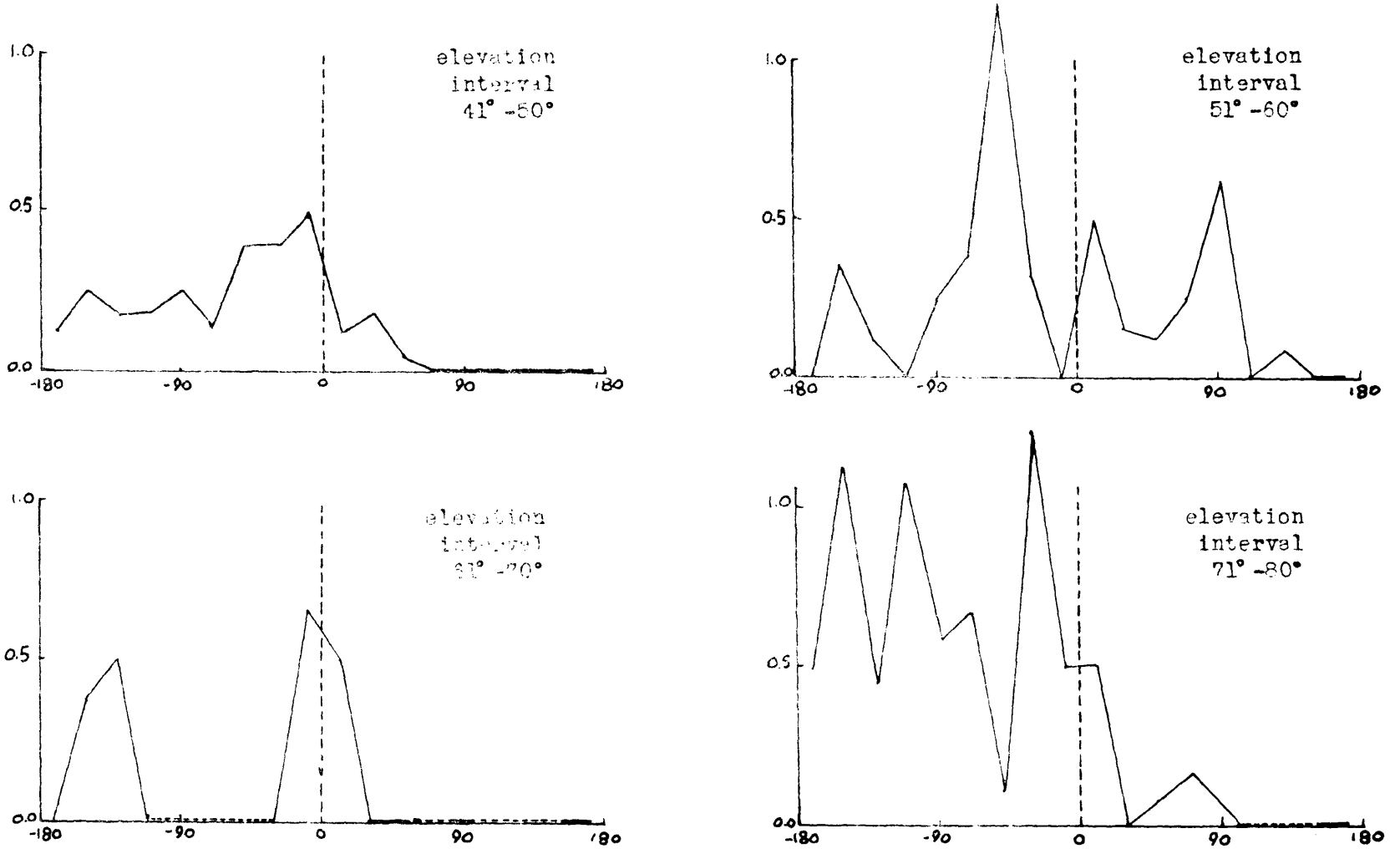

FIGURE 13B.- AVERAGE SCINTILLATION INDEX VERSUS AZIMUTH

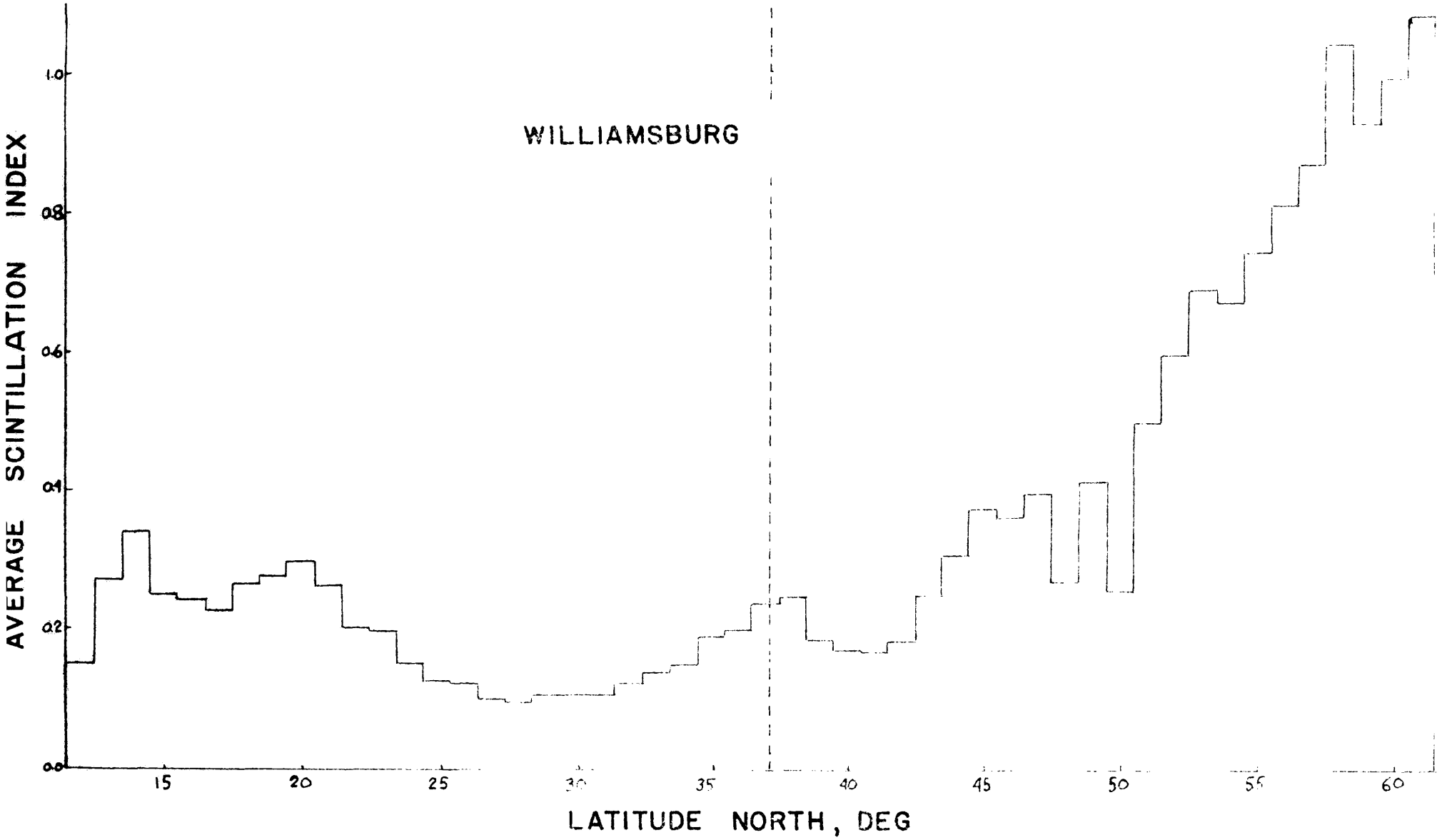

FIGURE 14. - AVERAGE SCINTILLATION INDEX VERSUS LATITUDE

CONCLUSIONS

The results of studying satellite scintillation as a function of satellite position strongly suggest certain properties which appear to be characteristic of the ionospheric irregularities responsible for scintillation. The dependence of scintillation upon elevation angle shown in Figures 10 and 11 agrees reasonably well with results of Lawrence[14], although he does not show the apparent increase in scintillation activity for high elevations. The fact that the scintillation index increases with decreasing elevation angle indicates that the ionospheric region in which the irregularities occur is relatively thick, i.e., the irregularities have an appreciable vertical distribution. If this is so, the part of the propagation path through the region of irregularities is longer when the satellite is near the horizon than when it is directly above the observer. If the region containing the irregularities were confined to a thin ionospheric layer, then the greater path length for low elevations would not be as important, and the dependence of scintillation index upon angle of elevation would be diminished.

The variation of scintillation activity with azimuth angle is particularly interesting. The well defined maximum of the scintillation index just to the west of true north strongly suggests that the ionospheric irregularities are influenced by the earth's magnetic field. According to Mawdsley[20] one might expect the region of high index to extend further south to the west of the observer than to the east if the irregularities which cause scintillation are elongated "blobs" aligned parallel to the magnetic field lines. This is precisely what is seen

is dependent upon the earth's magnetic field, but a more detailed description of the dependence is needed.

The probability is high that the overall picture of satellite scintillation is a composite result of a number of different effects. This is easily demonstrated by noting the elevation effect in the azimuthal and latitude studies. It seems possible that there exist irregularities in different ionospheric layers which cause scintillation to be observed at different times. A likely experiment would be a study of satellite scintillation during the hours near sunrise when the D region is being formed. The formation of a new ionization layer and the possible associated turbulence might give rise to irregularities which could produce scintillation.

REFERENCES

1. J.S. Hey, S. J. Parsons, and J.W. Phillips, Nature 158, 234 (1946).
2. F.G. Smith, Nature 165, 422 (1950).
3. G.C. Little and A.C.B. Lovell, Nature 165, 423 (1950).
4. H.G. Booker, Proc. Inst. Radio Engrs. 46, 298 (1958).
5. O.B. Slee, Nature 181, 1610 (1958).
6. K.C. Yeh and G.H. Swenson, J. Geophys. Research 64, 2281 (1959).
7. A.C. Aiken, "A Preliminary Study of Sunrise Effects in the D Region," Ionospheric Research Report No. 133, Penn State Univ. (1960).
8. M. Nicolet, Mem. Roy. Met. Inst. Bel. 19, 1 (1945).
9. J.A. Ratcliffe, Physics of the Upper Atmosphere (Academic Press, New York and London, 1960).
10. E.K. Smith, "Worldwide Occurrence of Sporadic E," Natl. Bur. Standards Circular 582 (1957).
11. S.K. Mitra, The Upper Atmosphere (The Asiatic Society, Calcutta, 1952).
12. E.V. Appleton, Proc. Inst. Radio Engrs. 47, 155 (1959).
13. J.C. Seddon, J. Geophys, Research 58, 323 (1953).
14. J.D. Lawrence, Dissertation, Univ. of Virginia (1960).
15. W.H. Stafford and R.M. Croft, NASA Tech. Note D-613 (1961).
16. Aviation Weekly 75, no. 2, p. 26 (July, 1961).
17. The Radio Amateur's Handbook (The American Radio Relay League, 1961), 38th edtn., 357.
18. S.A. Bowhill, J. Atmos, Terr. Phys. 13, 175 (1958).

19. W.J. Ross, "Ionospheric Investigation from Satellite Radio Observations, 1. Doppler Effect Recording Instrumentation," Ionospheric Research Report No. 120, Penn State Univ. (1959).

20. J. Mawdsley, J. Atmos. Terr. Phys. 18, 344 (1960).

21. G.S. Kent, J. Atmos. Terr. Phys. 16, 10 (1959).

22. J.B. Daniels and S.J. Bauer, J. Franklin Inst. 267, 187 (1959).

SCHEMATIC: FREQUENCY CONVERTER: 10-40 Mc

APPENDIX I

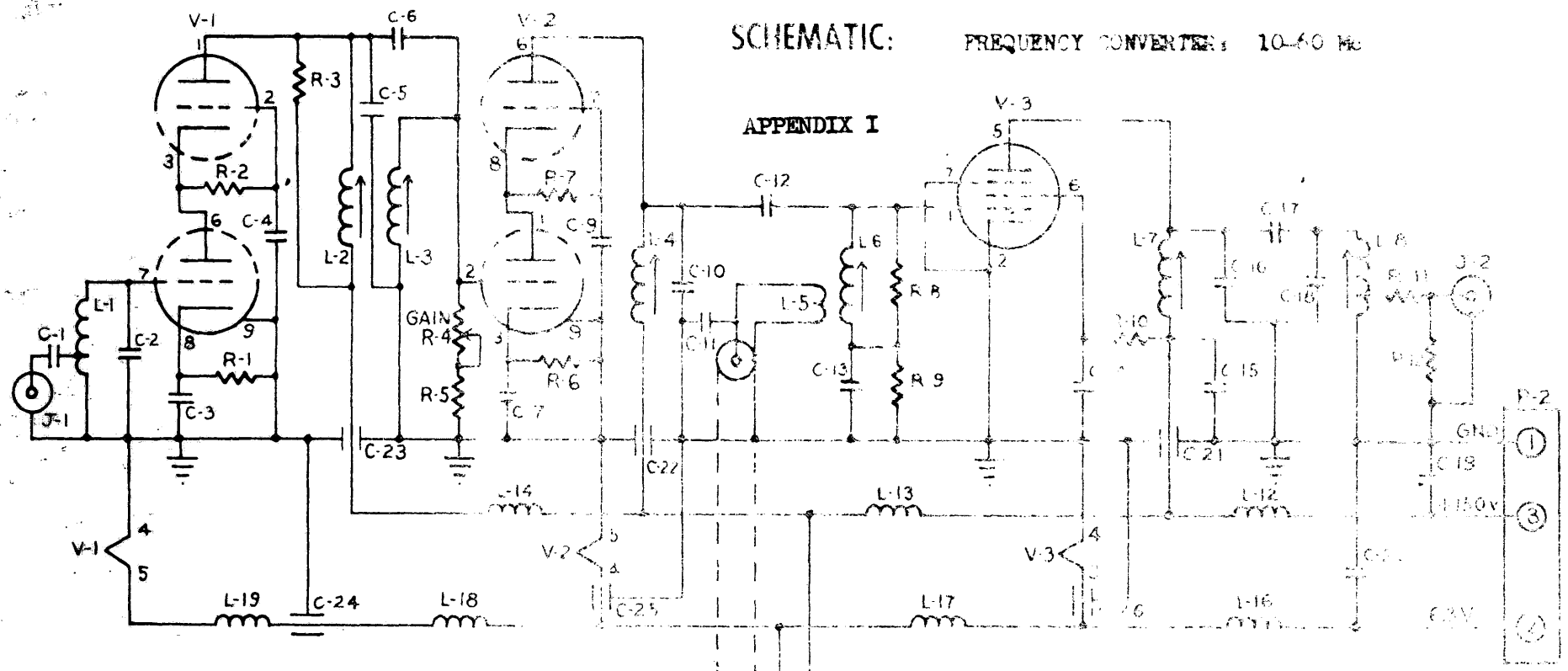

PARTS LIST

C-1 [illegible] 50 MMF
C-2 [illegible] MMF
C-3 [illegible] MMF
C-4 [illegible] MMF
C-5 [illegible] MMF
C-6 [illegible] MMF
C-7 .01 MMF
C-9 [illegible] MMF
C-10 82 MMF
C-11 3.5 MMF
C-12 THRU 23 [illegible]
C-24 [illegible]
C-25 [illegible]
C-30 27 MMF
C-31 [illegible]
C-32 [illegible]
C-33 [illegible]
L-1 THRU 12 [illegible]
L-13 [illegible]
L-14 [illegible]
L-16 [illegible]
L-17 [illegible]
L-18 [illegible]
L-19 [illegible]
L-20 [illegible]
L-21 [illegible]
P-1 [illegible]
P-2 [illegible]
R-1 [illegible]
R-2 [illegible] 1 MEG OHM
R-3 [illegible] 1 MEG OHM
R-4 [illegible] 5 K OHM
R-5 [illegible] 47K OHMS
R-6 [illegible]
R-7 [illegible]
R-8 [illegible]
R-9 [illegible]
R-10 [illegible]
R-11 [illegible]
R-12 [illegible]
R-13 [illegible]
R-14 [illegible]
R-15 [illegible]
R-16 [illegible]
R-17 [illegible]
V-1 6SA7
V-2 6SA7
V-3 6SB6
V-4 6AB4

NOTE: Optional Gain Control Adds The Following Parts
R-3 [illegible] OHM, R-4 5 K Ohm Gain Control Change R-5

APPENDIX II

Faraday Effect for Quasi-Longitudinal Propagation

When the angle between the direction of propagation and the magnetic field is less than 80° and the frequency is greater than 20 Mc/sec, the wave may be considered to be nearly circularly polarized.[22] The rotations of the ordinary and extraordinary waves having wavelengths λ_o and λ_e respectively are

$$\phi_o = 2\pi\, dr/\lambda_o \quad \text{and} \quad \phi_e = 2\pi\, dr/\lambda_e ,$$

where dr is an element of path length.

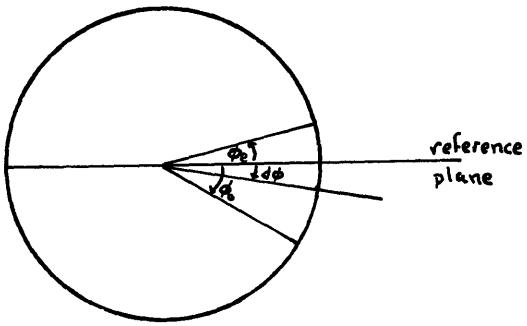

From the polarization diagram,

$$\phi_e + d\phi = \phi_o - d\phi$$

or
$$d\phi = \tfrac{1}{2}(\phi_o - \phi_e) , \qquad (1)$$

where $d\phi$ is the amount which the plane is rotated when the wave travels a distance dr. We may rewrite equation (1) in terms of the index of refraction n, if we express the rotations of the components by

$$\phi_i = 2\pi\, dr/\lambda_i = 2\pi(f/v_i)dr$$

$$= \omega(n_i/c)dr .$$

Then,
$$d\phi = (\omega/2c)(n_o - n_e)dr . \qquad (2)$$

When the transmitted frequency is much greater than the plasma frequency, the Appleton-Hartree equation for the indices of refraction becomes

$$n_{o,e}^2 = 1 - \frac{1}{\left(\frac{\omega}{\omega_N}\right)^2 - \frac{\omega_H^2}{2\omega_N^2}\sin^2\Theta \pm \frac{\omega\omega_H}{\omega_N^2}\left[\left(\frac{\omega_H \sin^2\Theta}{2\omega}\right) + \cos^2\Theta\right]^{1/2}}, \qquad (3)$$

where ω = angular frequency of transmitted wave

ω_N = angular plasma frequency

ω_H = angular gyromagnetic frequency, and

Θ = angle between the direction of propagation and the earth's magnetic field. We may make the approximation for quasi-longitudinal propagation provided

$$\frac{\omega_H}{2}\sin\Theta\tan\Theta \ll \frac{\omega^2 - \omega_N^2}{\omega} .$$

Then we may rewrite equation (3) in the form

$$n_{o,e} = \left\{1 - \left(\frac{\omega_N}{\omega}\right)^2 \Big/ \left[1 \pm \left(\frac{\omega_H}{\omega}\right)\cos\Theta\right]\right\}^{1/2}$$

$$\simeq 1 - \tfrac{1}{2}\left(\frac{\omega_N}{\omega}\right)^2\left[1 \mp \left(\frac{\omega_H}{\omega}\right)\cos\Theta\right] .$$

Hence, $$n_o - n_e = \frac{\omega_N^2\omega_H\cos\Theta}{\omega^3} .$$

We substitute $$\omega_N^2 = \frac{4\pi e^2 N}{m}$$

$$\omega_H = \frac{eB}{mc} ,$$

where N = electron number density (cm^{-3})

m = electron mass (gm)

e = electron charge (esu), and

B = earth's magnetic field (Gauss),

so that equation (2) becomes

$$d\phi = \frac{e^3 NB\cos\Theta}{2\,m^2c^2f^2}\,dr .$$

Finally,

$$\phi = \frac{e^3}{2\,m^2c^2f^2}\int_0^R NB\cos\Theta\,dr,$$

where ϕ gives the total rotation along the path from O to R. For the Faraday rotation of a satellite signal, we consider the origin of co-ordinates at an observer and integrate from the ground to a height h. Now,

$$\phi = Kf^{-2}\int_0^h B_L N(z)\ \sec\delta\ dz,$$

where $K = \dfrac{e^3}{2\ m^2c^2}$

$B_L = B\cos\theta$ = component of magnetic field in direction of propagation

δ = angle between ray path and the vertical (z-axis).

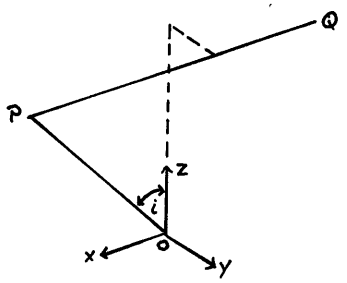

Let us assume that the satellite moves along a path PQ parallel to the x-axis with a constant velocity V at a constant height h always above the layers of maximum ionization in the ionosphere. If we assume a flat earth,

$$\phi = Kf^{-2}B_L N_T\ \sec(i),$$

where N_T = electron density / area column at height h

i = angle of incidence of ray.

Since the direction cosines of OP are x/OP, y/OP, z/OP, we may write B_L in terms of the field components

$$B_L = \frac{xB_x + yB_y + zB_z}{OP}.$$

Also, $\sec(i) = OP/h$.

Hence, $$\phi = Kf^{-2}N_T\left(\frac{xB_x + yB_y + zB_z}{h}\right).$$

We differentiate with respect to time to describe the polarization fading observed with a linearly polarized antenna.

$$\frac{d\phi}{dt} = V \frac{d\phi}{dx}$$

$$\simeq \frac{K'}{f^2} \frac{N_T B_z V}{h}.$$

Therefore, under the assumptions used, the Faraday fading of a satellite signal varies directly with the integrated electron density along the line of sight, directly with the component of the earth's magnetic field parallel to the satellite's motion, and inversely with the square of the transmitted frequency. (The results of the flat earth approximation are due to Bowhill.[18])

VITA

Joseph Kunkle Alexander, Jr.

Born in Staunton, Virginia, January 9, 1940. Graduated from Robert E. Lee High School in that city, June 1956; B. S.; College of William and Mary, 1960. Served with the National Bureau of Standards, Summer 1960. Returned to William and Mary as an M. A. candidate in Physics, September 1960.